Effects of Elevated CO2 on Morphological and Physiological Leaf Traits in Cabernet Sauvignon and Riesling

By

KAYLA ELMENDORF
THESIS

Submitted in partial satisfaction of the requirements for the degree of

MASTERS OF SCIENCE

in

Viticulture and Enology

in the

OFFICE OF GRADUATE STUDIES

of the

UNIVERSITY OF CALIFORNIA

DAVIS

Approved:

Elisabeth Forrestel, Chair

Andrew McElrone

Megan Bartlett

Committee in Charge

2023

Acknowledgements

Elisabeth Forrestel, Mina Momayyezi, Devin Rippner, Susanne Tittman, Guillaume Théroux Rancourt, Paige Breen, Paul Bringas, Manfred Stoll, Andrew McElrone, Christopher Muir, the lab, Geisenhiem, Swiss Light Source at the Paul Scherrer Institute, Department of Viticulture and Enology at University of California Davis, College of Agriculture and Environmental Science at University of California Davis.

Abstract

Atmospheric CO_2 has increased over the past several decades at a rate faster than all previous natural increases and is likely to increase by another 15% by 2050. Currently, impacts of elevated atmospheric CO_2 on growth, performance, and production in viticulture are not well understood and difficult to decouple from other climatic variations (e.g water availability and warming). This study was conducted in 2019 at the Free-Air Carbon dioxide Enrichment (FACE) at the University of Geisenheim established in 2012 to assess effects of elevated CO_2 (eCO_2) (+20%) on physiological, structural, and morphological responses of *Vitis vinifera* cv. Cabernet Sauvignon and Riesling. The baseline ambient CO_2 (aCO_2) was 411 ppm in 2019 while the eCO_2 treatment was 480 ppm. To evaluate the physiological effects, CO_2 response curves, leaf gas exchange measurements, and isotopic data were collected from elevated and ambient blocks. To assess the morphological effects, the same leaves used for gas exchange from ambient and elevated blocks were collected and scanned using X-ray microcomputed tomography (micro-CT) at Swiss Light Source. There were few significant differences between treatments on the parameters tested suggesting that, over time, there may be an acclimation effect of some Vitis vinifera species to moderate eCO_2.

Introduction

Human influence has caused the highest concentrations of atmospheric CO_2 in the last 2 million years (Allen et al. 1997). Since 1750, there has been a 40% increase in atmospheric CO_2 and projections predict that concentrations will likely increase another 20% to 40% within the century (IPCC, 2014). CO_2 is a vital component in photosynthesis that can influence various aspects of grapevine physiology, including gas exchange rates, leaf morphology, water use efficiency, and nutrient uptake. Currently, most wine growing regions are at the optimal climatic conditions for the grape varieties that are cultivated there (Jones et al., 2005). Globally, this amounts to a significant economic impact. In 2021, global annual production of grapes was 60 million tons (OIV, 2021) and the grape industry in California alone amounted to $5.33 billion (CDFA, 2021). Thus, a change in the morphophysiology of grapevines and subsequent effects on quality and yields of fruit would have tremendous implications. Cabernet Sauvignon and Riesling, specifically, are both popular wine grape varieties grown in many regions across the world that offer different anatomical origins to help describe different response tactics to environmental stressors such as eCO_2.

Some previous reports of elevated atmospheric CO_2 (eCO_2) levels in C3 crops show higher rates of photosynthesis (Ainsworth et al., 2002, Ainsworth & Rogers, 2007), plant biomass (Poorter & Navas, 2003), and yields (Ainsworth & Long, 2021; Kimball, 1983; Poorter et al. 2022) based on treatment. This suggests a positive correlation between eCO_2 and these traits; however, there is insufficient research to determine all of the impacts eCO_2 will have on grapevines, specifically. The development of free-air carbon dioxide Enrichment (FACE) systems has permitted exposure of plants to eCO_2 in fields without the confines of chamber walls. Confined chamber experiments

include temperature growth chambers (GC), greenhouse (GH), temperature gradient greenhouses (TGG), and open top chambers (OTC). Compared to other confined chamber experiments, FACE systems do a better job of capturing realistic plant responses (Long et al. 2005, 2006, Leakey et al. 2006) and enhance yield by ~50% less than in confined chamber studies (Long et al. 2005, 2006; Ainsworth and Long, 2005; Morgan et al., 2005). Thus, FACE experiments for grapevines are important for understanding their morphophysiological impacts.

Grapevine OTC, GH, TGG, and FACE experiments have reported increased photosynthesis (Anet) (Moutinho-Pereira et al. 2009, Martínez-Lüscher et al. 2015, Arrizabalaga-Arriazu et al. 2020, Wohlfahrt et al. 2018) and light saturated assimilation (Asat) (Edwards et al. 2016, 2017) with eCO_2 treatment. These are in-line with other C3 crop reports that have seen an increase in photosynthetic carbon assimilation (Ainsworth & Rogers, 2007; Long et al., 2004, Ainsworth & Long, 2021). However, there is also evidence for a down regulation of net photosynthesis as vines acclimate to higher carbon environments (Salazar-Parra et al. 2015, Rangel da Silva et al. 2017). A possible explanation for this observed downregulation is a lowered capacity of the photochemical machinery due to reductions in nitrogen (N) concentrations in the leaf (Luo et al. 1994, Moutinho-Pereira et al. 2009), limiting the activity of the rubisco enzyme (Clemens et al. 2021). Species that are not N fixing, such as grapevines, are more likely to experience down regulation in eCO_2 environments because of limited rubisco content (Ainsworth et al. 2002). Studies of other C3 plants have shown that, in general, leaves grown at eCO_2 show a decrease in the mass of N per unit dry mass (Koerner & Miglietta, 1994; McGuire et al. 1995; Drake et al. 1997).

Reported stomatal conductance responses to eCO_2 in C3 crops show general reductions (Ainsworth & Rogers, 2007; Long et al., 2004, Ainsworth & Long, 2021) whereas grapevines have shown variable results. While a FACE and enclosure study show a correlation between eCO_2 and decreased stomatal conductance (Bindi et al. 2005, Arrizabalaga-Arriazu et al. 2020), increased stomatal conductance in a FACE experiment has also been observed (Wohlfahrt et al. 2018). Grapevines can regulate stomatal conductance by adjusting the openness, size, and/or density of their stomata. Stomatal pore index (SPI) encapsulates size and density to help determine the conductance of gasses through stomata. Multiple studies have documented the reduction in stomatal density in several varieties of grapevine in response to eCO_2 (Moutinho-Pereira et al. 2009, Rogiers et al. 2011, Rangel da Silva et al. 2017).

Leaf water potentials also vary between studies. While an eCO_2 FACE experiment did not see differences in leaf water potentials even with decreases in stomatal conductance in the eCO_2 treatment (Bindi et al. 2005; Tognetti et al. 2005), another observed increased predawn leaf water potentials and stomatal conductance with the eCO_2 treatment (Wohlfahrt et al. 2018). This may suggest a morphological change to the leaves of vines over time or an interaction with soil water availability and root system development.

In FACE experiments, there have not been observed significant differences in plant phenology (Bindi et al. 2005). TGG experiments have observed both cultivar-dependent advancement of phenology (Martínez-Lüscher et al. 2016a) and non-significant differences in phenology by eCO_2 (Arrizabalaga-Arriazu et al. 2020). Open top chamber experiment found anthesis and veraison advanced only in the third season (Edwards et al. 2016, 2017)

FACE and GH experiments suggest an increase in vineyard fresh biomass as lateral leaf area and fresh weight of summer pruning by eCO_2 treatment (Bindi et al. 2001, Wohlfahrt et al. 2018, Kizildeniz et al. 2018) as well as yield and bunch architecture without an increase in number of bunches (Bindi et al. 2001, Wohlfahrt et al. 2018). However, even with these observed increases, there have been no significant effects on grape or wine quality in FACE nor OTC experiments. (Bindi et al. 2001, Gonçalves et al. 2008, Wohlfart et al. 2020, 2021). A GC experiment found a decrease in chlorophyll content (Pugliese et al. 2010), a GH experiment found no significant change in photosynthetic pigments (Salazar-Parra et al. 2012), and another GH experiment found increased chlorophyll a and b contents (Martínez-Lüscher et al. 2015).

Theoretical predictions and experimental observations have found that both the physical properties of the mesophyll (e.g., palisade and spongy mesophyll volume, porosity) and the underlying physiology (i.e., chloroplast positioning, aquaporins, and carbonic anhydrase activity) strongly influence CO_2 diffusion within a leaf and its concentration at the sites of carboxylation (Flexas et al., 2012; Momayyezi & Guy, 2017a, 2017b, 2018; Muir et al., 2014; Théroux‐Rancourt & Gilbert, 2017; Tholen & Zhu, 2011; Momayyezi et al. 2022). The ratio of palisade to spongy mesophyll volume within the leaf mesophyll affects photosynthetic efficiency, light adaptation, leaf structure and function, and water use efficiency. A higher proportion of palisade mesophyll can maximize light capture and photosynthetic rates, while an increased proportion of spongy mesophyll can enhance gas exchange and promote efficient carbon dioxide uptake. Porosity or the intercellular air spaces found between mesophyll cells facilitate gaseous exchange. After reaching the substomatal cavity, CO_2 molecules are subject to a series of gas and liquid phase resistances along the diffusion pathway through the intercellular airspace, cell walls, membranes, cytosol, and other cellular components to reach carboxylation

sites inside chloroplasts. The inverse of the sum of these resistances is used to calculate mesophyll conductance (gm) which can give insight into the movement of gasses throughout the leaf (Flexas et al., 2008; Flexas et al., 2018; Tosens & Laanisto, 2018, Momayyezi et al. 2022).

Understanding how Cabernet Sauvignon and Riesling acclimate to changing atmospheric conditions can help growers and winemakers make informed decisions about varietal selection and vineyard management techniques. Overall, studying elevated atmospheric CO_2 in these varieties provides valuable insights into the potential impacts of climate change on viticulture and helps predict changes in wine quality.

Methods

Field Site

Data were collected in 2019 at the VineyardFACE experiment site at the Hochschule Geisenheim (latitude: 49° 59’ N, longitude: 7° 57' E, elevation: 95 m) in the Rheingau winegrowing region of Germany. A detailed description of the field site has been described previously (Wohlfahrt et al. 2018). This site was 0.5 hectares planted in 2012 from one year old pot-grown vines of *Vitis vinifera* cv. Cabernet Sauvignon (CS) (clone 170) grafted on rootstock 161-49 Couderc and Riesling (R) (clone 198-30 Gm) grafted on rootstock SO4 (clone 47Gm). Rows were oriented north-south with a vine spacing of 0.9m within rows and 1.8m between rows. They were trained using a vertical shoot positioning system (VSP) with one year old canes pruned to 5 nodes per m^2 or approximately 8 nodes per vine. No other canopy manipulations took place. The vines were not irrigated; Geisenheim receives, on average, 446mm (17.56") of precipitation annually. Cover

crop consisted of Freudenberger WB 130 mulch mixture III, permanent vineyard greening I (Feldsaaten Freudenberger, Krefeld, Germany) in every second row. The cover crop mixture consisted of 5% perennial ryegrass, 30% creeping red fescue, 20% Kentucky bluegrass, 5% perennial ryegrass, 20% Chewing's fescue and 20% Kentucky bluegrass. The cover crop was mowed several times during the vegetation period.

VineyardFACE

The VineyardFACE experiment was designed as a randomized replicated treatment of three paired plot rings (Figure 1). Three rings were under ambient CO_2 (aCO_2, 411 ppm in 2019) and three moderately elevated CO_2 (eCO_2, +20% of the aCO_2 treatment). Each ring consisted of seven rows that alternated between CS and R. Nine vines per treatment for each variety was sampled (2 varieties x 2 treatments x 9 reps = 36 total vines). Each ring consists of 36 CO_2 towers 2.5m in height. Each tower contained a single blower (MP25/4T; CasaFan GmbH, Hasselroth, Germany) that created an airstream and one solenoid emitter that maintain carbon dioxide levels (Wohlfahrt et al., 2018). Wind direction and wind velocity were measured in real time by the transmitters (Thies GmbH, Goettingen, Germany) and were capable of immediately responding to environmental changes. At the center of each FACE-ring at 1.5m height, CO_2 was recorded using carbon dioxide transmitters (GMD20, Vaisala, Helsinki, Finland) to adjust CO_2 accumulation. CO_2 fumigation was maintained from sunrise to sunset 365 days a year since 2014, operated by an astronomical clock (Selektra 170 top2 Theben, Haigerloch, Germany). No CO_2 enrichment was carried out at wind velocity<0.1m s−1 or air temperatures<5°C. All measurements for this study were carried out on the same leaves for each plant per month of collection.

Field Measurements

Photosynthetic measurements

Net assimilation rate (An), stomatal conductance (gs) and the intercellular airspace CO_2 concentration (Ci) were measured consistently for the youngest fully developed leaves, 6-8 leaves for Vitis spp. using the plastochron index. Photosynthetic measurements were taken using a LI-COR 6800 system fitted with 6800-01A fluorometer. All measurements were done under photosynthetic photon flux density (PPFD) = 1500 (10% blue vs. 90% red) (µmol m-2 s-1), chamber temperature at 30°C, flow rate at 500 (µmol air s-1), and vapor pressure deficit between 1.5-2.0 kPa between 8:30 am to 1:30 pm. All leaves were dark adapted for 20 minutes prior to all other measurements to obtain the maximum quantum yield of photosystem II. The quantum yield of photosystem II (ΦPSII) under actinic light was obtained by application of saturating multiphase flashes (15000 µmol m-2 s-1) as per Genty et al. (1989). Leaves were light-adapted at PPFD = 1500 µmol m-2 s-1 for 10-15 minutes prior to photosynthetic measurements.

A-Ci curves

Photosynthetic measurements were CO_2 response (A_n-C_i) curves for each cultivar at 1500 µmol m^{-2} s^{-1} PPFD under the following sample CO_2 concentration: 400, 50, 80, 100, 150, 200, 250, 400, 500, 600, 700, 800, 900, 1200, 1400, 1600 ppm for both ambient and elevated CO_2 blocks.

Mesophyll conductance (g_m) calculation

Photosynthetic measurements concurrent with chlorophyll fluorescence were used to calculate mesophyll conductance (gm).

g_m - chlorophyll fluorescence method

The "constant *J* method" is commonly used to estimate g_m based on calculation of electron transport rate:

$$J_{flu} = \phi_{PSII} \times PPFD \times a \times \beta \qquad (1)$$

where β (0.5 for C_3 plants) is the fraction of absorbed quanta reaching photosystem II (Bernacchi *et al.,* 2002). The leaf absorbance, α, was measured to be 85.3% based on the average value (± 0.2 standard error) in all individuals using an ASD Fieldspec spectroradiometer (ViewSpec Pro, ASD Inc. Boulder, CO, USA). g_m was given by (Harley *et al.,* 1992):

$$g_m = A_n / [Ci - (\frac{\Gamma^*(J_{flu} + 8(A_n + R_d))}{J_{flu} - 4(A_n + R_d)})] \qquad (2)$$

where C_i is the intercellular airspace CO_2 concentration, R_d is the non-photorespiratory respiration rate in the light (unit: μmol m^{-1} s^{-1}), Γ^* is the chloroplast CO_2 photo compensation point (unit: μmol mol^{-1}), and A_n is the net assimilation rate. Γ* was assumed to equal the intercellular CO_2 photo compensation point (C_i^*) per Gilbert et al. (2012). Rd (0.77 ± 0.05 μmol m-2 s-1) and C_i^* (48.34 ± 0.30 μmol mol-1) were estimated using the Laisk method (Laisk, 1977 in Gilbert et al., 2012) as the point of intersection of the linear portion of averaged four sets of An-Ci curves obtained at two irradiances (125 and 500 μmol m-2 s-1) and 13 CO_2 concentrations (35, 40, 50, 60, 70, 80, 90, 100, 110, 120, 140, 160, and 180 μmol mol-1). Data for the Laisk method was acquired from a previous study on Cabernet Sauvignon at University of California, Davis (Supporting Information Fig. S1, Momayyezi, unpublished data). Having obtained gm by the chlorophyll fluorescence method, the CO_2 concentration in the chloroplast (C_c) was estimated according to Harley et al., (1992):

$$C_c = C_i - \frac{A_n}{g_m} \qquad (3)$$

MicroCT

For 164 leaves, we quantified from microCT images the volumes of spongy and palisade mesophyll cells as well as the intercellular airspace of the mesophyll cells.

Young fully expanded leaf leaves were collected, put on ice in sealed bags, and brought to the TOMCAT tomographic beamline of the Swiss Light Source at the Paul Scherrer Institute (Villigen, Switzerland). MicroCT imaging follows the protocol in Theroux-Rancourt et al. 2022. Within 24 hours of leaf collection, a thin strip of ~1.5 mm width and 1.5 cm length) was cut between second-order veins at the facility. Within 24 hours of leaf collection, a short strip (0.4 x 1.5 cm) was cut between second-order veins at the facility. The base of the strip was immediately wrapped in polyimide tape and inserted into a styrofoam block fixed on a sample holder. Three strips were cut at different locations on the leaf surface to ensure within-leaf replications and to get better leaf-level averages. The strip was immediately scanned by imaging 1801 projections of 100 ms under a beam energy of 21 keV and a magnification of 40x, yielding a final voxel size of 0.1625 µm (field of view: ~416x416x312 µm). Scanned projections were reconstructed to a transverse view using both absorption (gridrec; Marone *et al.* 2012) and phase contrast enhancement (Paganin *et al.* 2002) reconstruction. Protocols for processing microCT scans use freely available and open source software ImageJ (Schneider et al., 2012) and the Python programming language for machine-learning segmentation and for image analysis. Sampling methods followed the protocol described in (Théroux-Rancourt, 2020). The Python code was developed by (Rippner, 2022) and uses machine learning for the quantification of 3D leaf anatomical traits of grapevine (*Vitis vinifera* subsp. *vinifera* L.) which reduces the time required to process scan data into detailed segmentations.

Segmentation and FCN model

Between 400 and 500 consecutive slices from each grid stack were selected for manual segmentation using ImageJ software (Schneider et al., 2012) and a Wacom tablet. The resulting image stack was segmented using the methods presented by Momayyezi et al. (2022). Eight slices were manually masked for various leaf tissues per scan (three leaf scans per vine; 24 scans total). The manually-segmented slices had individual labels for the adaxial epidermis, abaxial epidermis, palisade mesophyll cells, spongy mesophyll cells, intercellular airspace, bundle sheath extensions, veins, and background outside of the scanned leaf. 28 masks and associated images were pulled together to run a "big model" using a fully convolutional network (FCN) model. 216 and 48 masks and images combos were used for training and testing FCN, respectively.

To verify auto-segmentation, intercellular airspace (IAS) trait, palisade mesophyll, and spongy mesophyll volume estimation by random forest model, a PyTorch implementation of FCN model with a ResNet-101 backbone was used for the semantic segmentation of the leaf image data with cloud-based resources in Google Colab. For training, we used a binary cross-entropy loss function, an Adam optimizer for stochastic optimization with a learning rate of 0.001, a scaling factor of 1 to avoid small feature loss in the training images, and a batch size of one to accommodate the GPU limitations in Google Colab.

Mesophyll porosity, palisade mesophyll and spongy mesophyll volume

Mesophyll porosity (θ_{IAS}; $m^3\ m^{-3}$) was calculated as the intercellular airspace (IAS) volume as a fraction of the total mesophyll volume as described by Momayyezi et al. (2022). The IAS volume (V_{IAS}) to palisade mesophyll and spongy mesophyll cell volume ($V_{palisade}$ and V_{spongy}) to whole mesophyll ratio (V_{mes}) were calculated as $V_{palisade}/\ V_{mes}$ ($m^3\ m^{-3}$) and $V_{spongy}/\ V_{mes}$ ($m^3\ m^{-3}$), respectively.

Stomatal Image Analysis

Stomatal pore area index (SPI), stomatal density, and stomatal length correlate to leaf gas exchange capacity. To measure leaf stomata, epidermal prints of the abaxial side were taken on the same leaves used for other parameters. First, the leaves were pressed and dried using a press plant. Dental putty was to take three imprints of three different sections of the leaves (n=213). Each section was about one inch from the center base of the leaf and spanned across, avoiding major veins. Under a fume hood, clear nail polish was used to take a second imprint of the putty resulting in a negative of a negative. Slides were made with the nail polish imprints. Images were taken of one field of view per leaf using a Leica DM 1000 compound microscope at 10x magnification with a scale bar attached to the image. Later, each image was analyzed using ImageJ to measure total stomatal counts and the lengths of 5 stomata. This was used to estimate stomatal density and average stomatal guard cell length. SPI was calculated as a product of stomatal density and the square of pore length and was calculated as SPI = stomatal length^2/ stomatal density.

Leaf Weight and Area

Each leaf was harvested for weighing and imaging at the University of Geisenheim. Fresh weights were taken the day of sampling. Images were taken using a scanner at 300 pixels per inch. Area was calculated using ImageJ. SLA was calculated from these parameters (Garneir et al. 2001).

Statistical analysis

Statistical analyses were performed with the statistical software RStudio, version 2022.12.0+353. Statistical analyses were done separately for June and August using two-way ANOVA tests examining the main effects of treatment and block. Statistically significant results of main factors on figures are indicated by * and ** ($p < 0.1$, $p < 0.01$). The complete code is stored on Github (https://github.com/forrestellab/FACESummer2019).

Results

Physiological traits

This study did not find any significant differences in Vcmax, Amax, SLA, SPI, nor mesophyll conductance (gm) by treatment. Jmax was significantly lower by treatment in Riesling in June (Fig 3B, $p= 0.0983$, $F= 3.213$). CO_2 response curves for both Cabernet Sauvignon and Riesling in both June and August are shown in Figure 2. There is a slight deviation between CO_2 treatment in the August Riesling ACi curves.

Morphological traits

The fraction of palisade cell volume in total mesophyll volume was significantly higher by treatment in June for Cabernet Sauvignon (Fig 4A, $p=0.0968$, $F=3.069$) and lower by eCO_2 treatment in August for Riesling (Fig 4A, $p=0.0071$, $F=8.274$).

The fraction of spongy cell volume in total mesophyll volume was significantly lower by treatment in August for both Cabernet Sauvignon (Fig 4B, p= 0.0852, F= 3.169) and Riesling (Fig 4B, p= 0.0127, F=6.967).

Discussion

The rate that atmospheric CO_2 has risen in the last few decades has surpassed that of all previous natural increments, and it's anticipated that it could grow by an additional 15% from its current levels, reaching 480 ppm by 2050. Literature suggests that there is a fertilization effect with eCO_2 meaning that plants increase their photosynthetic abilities and shift physiological and morphological responses (Ueyama et al. 2020). However, as described by the model presented by Sage 1990, non-limiting processes of photosynthesis could be regulated in C3 plants to balance the capacity of limiting processes. For instance, when CO_2 levels are elevated, and the electron transport or phosphate regeneration may limit photosynthesis, the activity of rubisco is downregulated to balance the limitation in RuBP regeneration (Clemens et al. 2021). Elevated CO_2 levels can influence uptake, allocation, and efficiency, which can also potentially exacerbate nitrogen limitations. This phenomenon is supported by findings Luo et al. 1994, Moutinho-Pereira et al. 2009 and Rangel da Silva et al. 2017 which all report reductions in leaf nitrogen concentrations by eCO_2 treatment. This study, however, has found few significant differences in morphological and physiological measurements by treatment in both time points and thus does not find strong evidence for the downregulation of nitrogen levels. Nitrogen levels were not directly assessed in this study. Although research done in previous years on the same blocks did not find significant differences in leaf nitrogen content (Wohlfahrt et al. 2022),

nutrient status can change dramatically over time. The ability of plants to respond effectively to eCO_2 in the future will undoubtedly rely on physiological attributes such as their efficiency in utilizing nitrogen and water, their photosynthetic capabilities, their capacity to serve as sinks for resources, and their structural adaptations (Diaz 1995).

Maximum assimilation rate

Maximum assimilation rate (Amax) signifies a leaf's peak capacity to absorb CO_2 per area and time during photosynthesis. The prevailing hypothesis suggests that eCO_2 acts as a growth stimulant by providing a surplus of CO_2, the primary substrate for photosynthesis (Moutinho-Pereira et al. 2009, Martínez-Lüscher et al. 2015, Edwards et al. 2016, 2017, Wohlfahrt et al. 2017, 2018, Arrizabalaga-Arriazu et al. 2020). This surplus could lead to higher Amax, driving efficient carbon assimilation and potentially fostering increased plant growth and water use efficiency. This study, however, did not observe any significant differences in Amax by treatment (Table 2).

Jmax

Jmax refers to the maximal capacity of the photosynthetic electron transport chain, which is a critical process in photosynthesis. It's responsible for generating energy-rich molecules like ATP and NADPH that are essential for carbon fixation. The prediction that Jmax could decrease with eCO_2 is based on the idea that increased CO_2 concentrations leads to a reduction in the demand for electron transport, as CO_2 availability might become less limiting (Ainsworth and Rogers 2007). This study only observed a significant difference by treatment in Riesling in June. Otherwise, there are no significant differences (Table 2).

Vcmax

Vcmax represents the maximal rate at which the enzyme Rubisco can catalyze the carboxylation of ribulose-1,5-bisphosphate during photosynthesis. The assumption that Vcmax could decrease under eCO_2 comes from the idea that elevated CO_2 levels lead to an upregulation of the photosynthetic system, reducing the need for a higher Vcmax (Ainsworth and Rogers 2007). This study observed no significant differences by treatment (Table 2).

Stomatal Pore Index

Stomatal Pore Index (SPI), or the stomatal pore area per leaf area, is a key physiological parameter reflecting the balance between water-saving strategies and efficient gas exchange, holding crucial implications for plant adaptation, water use efficiency, and response to changing environmental conditions. A possible consequence of an eCO_2 might be an increase in the length of the stomatal aperture (length between the junctions of the guard cells at each end of the stomata), which might contribute to counteract a reduced stomatal density in response to high CO_2 levels (Ogaya, 2011). As described in Pritchard et al. 1999, previous studies have observed increases, decreases, and also no changes of stomatal density in C3 plants in response to eCO_2. Experiments specifically studying grapevines, however, have generally observed a reduction in stomatal density to eCO_2 treatments (Moutinho-Pereira et al. 2009, Rangel da Silva et al. 2017). This study shows no significant differences in SPI by treatment (Table 2).

Mesophyll conductance

Mesophyll conductance (gm) gauges CO_2 diffusion efficiency from intercellular spaces to chloroplast stroma, involving cell layers (Mizokami et al. 2019). It's anticipated to decrease with eCO_2 (Mizokami et al. 2019). This stems from surplus CO_2 potentially prompting stomatal closure, diminishing the CO_2 pressure gradient. This study, however, shows no significant differences in gm by treatment (Table 2). These results align with the insignificant differences in SPI by treatment.

Specific Leaf Area

Specific Leaf Area (SLA) refers to the leaf area of a plant divided by its dry mass, and it's often used as an indicator of resource allocation strategies. SLA reflects how plants allocate resources between structural support (leaf mass) and light-interception surface area (leaf area). Higher SLA values prioritize light capture over leaf longevity, while lower SLA values invest more in structural support and leaf longevity. The prediction that SLA could increase under eCO_2 treatment is based on the idea that plants exposed to higher levels of atmospheric CO_2 might allocate more resources to light-interception surface area (Pritchard et al. 1999). The rationale behind this prediction is that eCO_2 is often associated with an increase in photosynthetic rates. As plants take in more CO_2, they might generate more energy, leading to greater allocation of resources to growth, including leaf expansion. Thinner leaves (higher SLA) are often observed in environments with ample resources, as they can optimize light capture for photosynthesis (Poorter et al., 2022, Arrizabalaga-Arriazu et al. 2020). This experiment, however, shows no significant differences in SLA by treatment in this experiment (Table 2).

Morphological Traits

Plant morphological adaptations to rising global CO_2 levels may prove to be critical due to the importance of plant form in the acquisition of resources, as a determinant of plant competitive interactions, and as a modifier of metabolic processes (Pritchard et al. 1999). There have been few papers assessing the effects of eCO_2 on the morphology of C3 plants with inconsistent findings in the papers that have been published. Pirchard et al. 1999 reports inconsistent findings in C3 plant's mesophyll cross-sectional areas of leaves with increased, decreased, and unchanged total measurements by eCO_2 treatment. They concluded that effects of eCO_2 vary depending on the stage of leaf development, genetic plasticity, nutrient availability, temperature, and phenology. Wohlfahrt et at. 2022 used histological analysis of leaf cross-sections and found a significant increase in palisade mesophyll under eCO_2 but insignificant changes in spongy mesophyll. Thus, we predict the fraction of palisade cell volume in total mesophyll volume to increase, the fraction of spongy cell volume in total mesophyll volume to remain unaffected, and the fraction of intercellular air space volume in total mesophyll volume (Porosity) to decrease with eCO_2 treatment (Pritchard et al. 1999, Théroux-Rancourt et al. 2021, Wohlfahrt et at. 2022). Spongy mesophyll cells are a type of plant leaf cell that is involved in gas exchange, particularly facilitating the movement of gasses within the leaf. Based on Wohlfahrt et at. 2022's findings, we did not expect to see any significant differences. We, however, saw significant decreases for both varieties in August (Table 2; Figure 4) meaning the vines were allocating more resources into cells to facilitate gas movement later in the season. Palisade mesophyll, on the other hand, is primarily responsible for capturing light and conducting photosynthesis. A structural alteration can either enhance or diminish light absorption and utilization, thereby influencing the capacity to capitalize on the additional CO2 available for photosynthesis, either amplifying or reducing it. In this study, we observed an increase in the fraction of palisade cell volume in total mesophyll

volume by treatment in Cabernet Sauvignon in June and a decrease in Riesling in August (Table 2; Figure 4). Changes to leaf morphology in a single growing season could be a stress response to other factors. Reasons for why there are differences between varieties should be studied further. Porosity or the intercellular air spaces found between mesophyll cells facilitate gaseous exchange through the leaf. With eCO2, it is anticipated that porosity may decrease since the greater availability of CO2 allows for easier diffusion without encountering spatial limitations. In this experiment, however, we observed an increase in Riesling in August (Table 2; Figure 4). This finding correlates with a decrease in both the fraction of spongy cell volume in total mesophyll volume and the fraction of palisade cell volume in total mesophyll volume and without any significant differences in any of the physiological responses measured.

Previous VineyardFACE Research

Previous VineyardFACE studies conducted by Wohlfahrt et al. 2018, 2020, 2021 and 2022 found significant differences for various metrics in both cultivars and seasons. Wohlfahrt et al. 2018, 2020, and 2021 conducted research in 2014-2016 and Wohlfahrt et al. 2022 conducted research in 2015 and 2016. Wohlfahrt et al. 2018 found that both Riesling and Cabernet Sauvignon had higher photosynthetic rates as well as increased leaf and fruit biomass production. This effect was particularly evident in single berry weight, cluster weight and bunch architecture. Net assimilation increased, intrinsic water use efficiency improved, and transpiration rate and stomatal conductance were found to be higher under eCO_2 for both cultivars for all three years. Wohlfahrt et al. 2020 and 2021 found that eCO_2 altered some bunch and berry parameters without a negative impact on fruit quality nor the composition of must and young wines. Wohlfahrt et al. 2022's findings are the most in line with the parameters measured in this study.

They found that net assimilation rates were significantly stimulated under eCO_2 for both cultivars and seasons. Using leaf histological analysis of leaf cross-sections, they found a significant increase in palisade mesophyll and decreases in epidermal tissues in Cabernet Sauvignon. This compliments this study's findings of an increase in Cabernet Sauvignon the fraction of palisade cell volume in total mesophyll volume in June. Additionally, they found a significant increase in the ratio between palisade and spongy mesophyll in Cabernet Sauvignon under eCO_2. Total leaf thickness and width of spongy mesophyll of Cabernet Sauvignon and Riesling remained less affected under eCO_2 conditions. There were no impacts found in chlorophyll content nor lead to changes in other leaf pigments or leaf nitrogen status. They suggest, however, that the two cultivars within the VineyardFACE may decrease in leaf nitrogen under eCO_2 in future as variations in nitrogen content are also depending on the initial nitrogen limitation status of the single plant. Thus, the disparity in results between Wohlfahrt et al. 2018, 2020, 2021 and 2022 and this study may be due to nitrogen levels acting as an underlying restraint for physiological capacities and morphological development. While both this study and those of Wohlfahrt yielded statistically significant results, they were generally of marginal significance. It is possible that the moderately elevated CO2 treatment or +20% may not have been sufficiently robust to generate significant outcomes. Alternatively, over time, the vines might have acclimated to the eCO2 conditions. While previous investigations by Wohlfahrt et al. were conducted on the vines in 2015 and 2016 (when they were 4 and 5 years old, with 3 and 4 years of treatment, respectively), out study took place in 2019 when the vines had reached 8 years of age, with 7 years of treatment. Our proposition is that these vines have undergone an acclimation effect, suggesting that, given time, they are able to adapt to eCO2 levels. Another potential explanation for the inconsistencies in results could be attributed to seasonal variations and the timing of sample

collection. Previously, Wohlfahrt 2018 and 2022 noted seasonal differences between measurements taken in 2015 and 2016. It is possible that the weather conditions in 2019 could have contributed to fewer significant differences. Data from weather stations at University of Geisenheim should be consulted for a more comprehensive analysis. This study found significant differences between sampling dates for almost every parameter measured. Leaf age can significantly affect photosynthesis due to the changing physiological and structural characteristics of leaves as they mature (Schultz 2003). Furthermore, it is important to underscore that each grapevine variety was planted on a distinct rootstock, potentially accounting for some of the variability observed in their responses to eCO2 treatment.

Possible Reporting Bias

In this experiment, we examined the effects of a 20% increase in CO2 levels, a scenario anticipated for the mid-century. In the broader context of literature, this increase is thought to have a CO_2 fertilization effect on C3 plants. However, the findings of Haworth et al. 2016 suggests that this effect might be magnified due to reporting bias. Consequently, this paper suggests there is a scarcity of published research depicting outcomes that are statistically insignificant in response to eCO2 treatment. This potential distortion raises questions about the accuracy of attributing the observed CO_2 fertilization effect as an accurate representation of plant responses.

For a comprehensive understanding of these physiological and morphological processes, it is also crucial to consider how other stressors like heat, drought, pests, and diseases will negatively affect grapevine growth in combination with eCO_2. The compounding impacts of these

multifaceted environmental factors are likely to have a more profound impact on grapevine function compared to their individual influences (Clemens et al. 2021). Additionally, the potential limitations of confined chamber experiments such as GC, GH, and TGG should continue to be studied.

Conclusion

Limited morphological and physiological differences were found by eCO_2 treatment in *Vitis vinifera* cv. Cabernet Sauvignon and Riesling in this study. These results may indicate an intrinsic ability of grapevines to acclimate to eCO_2 conditions, raise questions about whether the treatment magnitude was substantial enough to elicit noticeable effects, or highlight the possible influence of additional unexplored variables inherent to this experimental design. The diverse responses observed among grapevines to eCO2 underscore the necessity for further research, particularly focusing on mature grapevines. Moreover, future research endeavors should take into account plant nutrient levels and comprehensive weather data to gain a more comprehensive understanding of these complex interactions.

Tables

Table 1. Description and abbreviations of plant traits used

Abbreviation	Variable Name	Units	Explanation	Hypothesized effect by treatment	References
Amax	Maximum Assimilation rate	µmol m-2s-1	Amount of CO_2 assimilated per leaf area and time	Predicted increase	Moutinho-Pereira et al. 2009, Martínez-Lüscher

					et al. 2015, Edwards et al. 2016, 2017, Wohlfahrt et al. 2017, 2018, Arrizabalaga-Arriazu et al. 2020
Ca	Ambient (to leaf) CO_2	µmol m-1		Predicted increase	Martínez-Lüscher et al. 2015
Ci	Intercellular CO_2	µmol m-1		Predicted increase	Martínez-Lüscher et al. 201522
Ci/Ca	Intercellular [CO_2] relative to outside the leaf	mol mol1	Measured with increasing CO_2 within chamber		Poorter et al. 2022
gm	Mesophyll Conductance	mol CO_2 m-2s-1	Measured using fluorescence; reflects the CO_2 diffusion pathway	Predicted decrease	Harley et al. 1992, Mizokami et al. 2019, Momayyezi et al. 2022
Jmax	Maximum Electron Transport Rate	µmol m-2s-1		Predicted to decrease	Ainsworth and Rogers 2007
$V_c$max	Maximum Carboxylation Rate	µmol m-2s-1		Predicted to decrease	Ainsworth and Rogers 2007
SLA	Specific leaf area	m2 kg1	Leaf area/leaf mass	Predicted to increase	Poorter et al., 2022, Arrizabalaga-Arriazu et al. 2020
SPI	Stomatal Pore Index		Stomatal pore area per leaf area; a proxy for leaf gas exchange capacity and thus water lost to transpiration	Unknown, but predicted to decrease	Pritchard et al. 1999, Moutinho-Pereira et al. 2009, Rangel da Silva et al. 2017

SL	Stomatal Length	µm	Length of guard cells	Unknown	
SD	Stomatal Density	Count per µm^2	Number of stomata per unit area	Predicted to decrease	Moutinho-Pereira et al. 2009
gs	Stomatal Conductance	mol m^-2 s^-1	Gas exchange through stomata	Predicated to decrease	Poorter et al. 2022, Leakey et al. 2012, Ainsworth EA, Rogers A. 2007
VoFrSp	Fraction of spongy cell volume in total mesophyll volume	`ml ml-1`	Spongy mesophyll volume/total mesophyll volume	Unknown	Pritchard et al. 1999, Momayyezi et al. 2022, Théroux-Rancourt et al. 2021, Wohlfahrt et at. 2022
VoFrPa	Fraction of palisade cell volume in total mesophyll volume	`ml ml-1`	Palisade mesophyll volume/total mesophyll volume	Predicted to increase	Pritchard et al. 1999, Poorter et al. 2022, Momayyezi et al. 2022, Théroux-Rancourt et al. 2021, Wohlfahrt et at. 2022
Porosity	Fraction of intercellular air space volume in total mesophyll volume	`ml ml-1`	Intercellular air space/total mesophyll volume	Predicted to decrease	Momayyezi et al. 2022, Earles et al. 2018, Théroux-Rancourt et al. 2021

Table 2. Two-way ANOVA tests by treatment (CO_2 Level), block, and vine (if applicable). *, **, ***, and **** indicate statistical significance (p <0.1, p < 0.05, p<0.01, p<0.001)

				Df	Sum Sq	Mean sq	F value	Pr(>F)

Stomatal Length	June	Cabernet Sauvignon	CO_2 Level	1	3.325	3.325	7.789	0.00867***
			Block	4	2.286	0.572	1.339	0.27617
			Vine	12	10.65	0.887	2.079	0.04782**
		Riesling	CO_2 Level	1	0.16	0.1579	0.152	0.6986
			Block	4	6.37	1.5921	1.536	0.2124
			Vine	12	29.22	2.4348	2.35	0.0238**
	August	Cabernet Sauvignon	CO_2 Level	1	0.319	0.3189	0.759	0.389
			Block	4	2.203	0.5508	1.311	0.285
			Vine	12	11.148	0.929	2.211	0.033**
		Riesling	CO_2 Level	1	0.277	0.2774	0.961	0.334
			Block	4	1.577	0.3942	1.366	0.265
			Vine	12	17.326	1.4439	5.002	0.0000811****
Stomatal Density	June	Cabernet Sauvignon	CO_2 Level	1	2.14E-10	2.14E-10	2.353	0.135
			Block	4	4.77E-09	1.19E-09	13.108	0.0000017****
			Vine	12	8.66E-09	7.21E-10	7.934	0.00000109****
		Riesling	CO_2 Level	1	2.22E-10	2.22E-10	1.35	0.253
			Block	4	1.19E-08	2.99E-09	18.129	0.0000000309****
			Vine	12	1.65E-08	1.38E-09	8.347	0.000000318****
	August	Cabernet Sauvignon	CO_2 Level	1	1.60E-09	1.60E-09	8.282	0.00669***
			Block	4	1.22E-08	3.05E-09	15.762	0.000000153****
			Vine	12	1.36E-08	1.13E-09	5.843	0.0000173****

		Riesling	CO_2 Level	1	1.04E-09	1.04E-09	2.094	0.1565
			Block	4	6.95E-09	1.74E-09	3.495	0.0164**
			Vine	12	3.76E-08	3.13E-09	6.304	0.00000776****
SPI	June	Cabernet Sauvignon	CO_2 Level	1	6.49E+10	6.49E+10	2.357	0.1317
			Block	4	4.46E+11	1.11E+11	4.048	0.0069***
		Riesling	CO_2 Level	1	1.77E+10	1.77E+10	0.124	0.7262
			Block	4	1.80E+12	4.50E+11	3.166	0.0218**
	August	Cabernet Sauvignon	CO_2 Level	1	3.96E+09	3.96E+09	0.173	0.68
			Block	4	2.13E+11	5.31E+10	2.313	0.071*
		Riesling	CO_2 Level	1	4.60E+10	4.60E+10	0.88	0.353
			Block	4	3.55E+11	8.88E+10	1.699	0.166
Area	June	Cabernet Sauvignon	CO_2 Level	1	11.5	11.5	0.844	0.376
			Block	4	144.1	36.02	2.644	0.086*
		Riesling	CO_2 Level	1	58.7	58.72	2.174	0.166
			Block	4	33.6	8.39	0.311	0.865
	August	Cabernet Sauvignon	CO_2 Level	1	0.03	0.027	0.002	0.967
			Block	4	38.12	9.531	0.631	0.65
		Riesling	CO_2 Level	1	4.32	4.318	0.362	0.559
			Block	4	46.17	11.543	0.968	0.463
Weight	June	Cabernet Sauvignon	CO_2 Level	1	1879	1879	0.056	0.8171

			Block	4	442789	110697	3.292	0.0486**
		Riesling	CO_2 Level	1	31668	31668	0.368	0.555
			Block	4	46863	11716	0.136	0.966
	August	Cabernet Sauvignon	CO_2 Level	1	8477	8477	0.19	0.671
			Block	4	39542	9885	0.221	0.921
		Riesling	CO_2 Level	1	68958	68958	1.429	0.255
			Block	4	98720	24680	0.511	0.729
Porosity	June	Cabernet Sauvignon	CO_2 Level	1	1.17E-06	1.17E-06	2.558	0.1271
			Block	4	6.71E-06	1.68E-06	3.656	0.0238**
			Vine	6	4.17E-06	6.95E-07	1.515	0.2293
		Riesling	CO_2 Level	1	9.20E-07	9.20E-07	0.802	0.38105
			Block	4	2.77E-05	6.93E-06	6.043	0.00234***
			Vine	9	1.52E-05	1.69E-06	1.475	0.22381
	August	Cabernet Sauvignon	CO_2 Level	1	2.06E-06	2.06E-06	2.684	0.112
			Block	4	1.64E-06	4.09E-07	0.533	0.713
			Vine	12	1.60E-05	1.33E-06	1.735	0.108
		Riesling	CO_2 Level	1	1.42E-06	1.42E-06	8.076	0.00774***
			Block	4	2.00E-07	4.99E-08	0.284	0.88587
			Vine	12	1.32E-06	1.10E-07	0.627	0.80387
VoFrPa	June	Cabernet Sauvignon	CO_2 Level	1	2.98E-07	2.98E-07	3.069	0.0968*
			Block	4	1.27E-06	3.16E-07	3.252	0.0358**
			Vine	6	7.59E-07	1.26E-07	1.3	0.3068
		Riesling	CO_2 Level	1	1.68E-07	1.68E-07	0.688	0.41651
			Block	4	6.31E-06	1.58E-06	6.471	0.00164***
			Vine	9	3.52E-06	3.91E-07	1.605	0.18082

	August	Cabernet Sauvignon	CO_2 Level	1	4.74E-07	4.74E-07	2.177	0.1505
			Block	4	4.63E-07	1.16E-07	0.531	0.7137
			Vine	12	4.88E-06	4.07E-07	1.869	0.0811*
		Riesling	CO_2 Level	1	4.61E-07	4.61E-07	8.274	0.0071***
			Block	4	7.29E-08	1.82E-08	0.327	0.8577
			Vine	12	6.22E-07	5.18E-08	0.93	0.5306
VoFrSp	June	Cabernet Sauvignon	CO_2 Level	1	2.88E-07	2.88E-07	2.092	0.1652
			Block	4	2.20E-06	5.51E-07	3.999	0.0171**
			Vine	6	1.41E-06	2.35E-07	1.707	0.1766
		Riesling	CO_2 Level	1	3.02E-07	3.02E-07	0.894	0.35571
			Block	4	7.61E-06	1.90E-06	5.631	0.00333***
			Vine	9	4.19E-06	4.66E-07	1.378	0.26209
	August	Cabernet Sauvignon	CO_2 Level	1	5.58E-07	5.58E-07	3.169	0.0852*
			Block	4	3.90E-07	9.76E-08	0.554	0.6975
			Vine	12	3.28E-06	2.73E-07	1.552	0.1604
		Riesling	CO_2 Level	1	2.61E-07	2.61E-07	6.967	0.0127**
			Block	4	5.99E-08	1.50E-08	0.399	0.8076
			Vine	12	2.41E-07	2.01E-08	0.535	0.8754
$V_c$max	June	Cabernet Sauvignon	CO_2 Level	1	0.7	0.72	0.009	0.9267
			Block	4	1066.4	266.61	3.275	0.0534*
		Riesling	CO_2 Level	1	146	146	1.142	0.306
			Block	4	949	237.3	1.856	0.183
	August	Cabernet Sauvignon	CO_2 Level	1	194.2	194.17	2.735	0.126
			Block	4	270.5	67.63	0.952	0.47
		Riesling	CO_2 Level	1	295.2	295.2	2.184	0.165

			Block	4	115	28.74	0.213	0.926
Jmax	June	Cabernet Sauvignon	CO_2 Level	1	0	0.4	0.001	0.9737
			Block	4	7972	1992.9	5.057	0.0147**
		Riesling	CO_2 Level	1	2404	2404.4	3.213	0.0983*
			Block	4	7176	1794	2.398	0.1081
	August	Cabernet Sauvignon	CO_2 Level	1	6	5.9	0.013	0.912
			Block	4	778	194.4	0.423	0.789
		Riesling	CO_2 Level	1	1583	1583.5	2.186	0.165
			Block	4	920	229.9	0.318	0.861
Amax	June	Cabernet Sauvignon	CO_2 Level	1	2.01	2.01	0.179	0.6804
			Block	4	165.78	41.44	3.697	0.0383**
		Riesling	CO_2 Level	1	17.39	17.39	0.917	0.357
			Block	4	168.54	42.13	2.221	0.128
	August	Cabernet Sauvignon	CO_2 Level	1	1.66	1.662	0.087	0.774
			Block	4	22.75	5.687	0.297	0.874
		Riesling	CO_2 Level	1	22.6	22.6	1.008	0.335
			Block	4	84.39	21.1	0.941	0.473
Gm	June	Cabernet Sauvignon	CO_2 Level	1	0.00846	0.008463	1.258	0.286
			Block	4	0.02607	0.006517	0.969	0.463
		Riesling	CO_2 Level	1	0.03153	0.031531	1.503	0.246
			Block	4	0.01665	0.004161	0.198	0.934
	August	Cabernet Sauvignon	CO_2 Level	1	0.00112	0.001115	0.043	0.839
			Block	4	0.01944	0.00486	0.188	0.94
		Riesling	CO_2 Level	1	0.05216	0.05216	2.826	0.121
			Block	4	0.00914	0.00229	0.124	0.971

SLA	June	Cabernet Sauvignon	CO_2 Level	1	6.78E-06	6.79E-06	1.207	0.293
			Block	4	4.67E-05	1.17E-05	2.078	0.147
		Riesling	CO_2 Level	1	8.80E-06	8.80E-06	1.041	0.328
			Block	4	2.68E-05	6.71E-06	0.793	0.552
	August	Cabernet Sauvignon	CO_2 Level	1	1.25E-05	1.25E-05	0.702	0.418
			Block	4	2.70E-05	6.75E-06	0.379	0.819
		Riesling	CO_2 Level	1	1.05E-05	1.05E-05	1.245	0.288
			Block	4	2.68E-05	6.70E-06	0.795	0.553

Table 3. Mean and standard errors

	Month	**CO_2 Level**	**Variety**	**Mean**	**SE**
Stomatal Length	June	ambient	Cabernet Sauvignon	8.166481	0.1749944
			Riesling	8.1675	0.3078824
		elevated	Cabernet Sauvignon	7.646296	0.1791341
			Riesling	8.283704	0.2017144
	August	ambient	Cabernet Sauvignon	7.036296	0.2015147
			Riesling	7.555926	0.1939548
		elevated	Cabernet Sauvignon	7.19	0.1456107
			Riesling	7.699259	0.2233767
Stomatal Density	June	ambient	Cabernet Sauvignon	9.41E-05	6.04E-06
			Riesling	8.69E-05	9.72E-06
		elevated	Cabernet Sauvignon	8.90E-05	5.32E-06
			Riesling	8.28E-05	6.11E-06
	August	ambient	Cabernet Sauvignon	1.18E-04	7.66E-06

			Riesling	1.22E-04	1.18E-05
		elevated	Cabernet Sauvignon	1.29E-04	7.77E-06
			Riesling	1.31E-04	8.25E-06
SPI	June	ambient	Cabernet Sauvignon	746924.7	40461.86
			Riesling	941643.2	84693.7
		elevated	Cabernet Sauvignon	675569.3	32869.94
			Riesling	905486	71543.9
	August	ambient	Cabernet Sauvignon	448085.4	29515.31
			Riesling	543652.7	54172.82
		elevated	Cabernet Sauvignon	430952.4	31654.02
			Riesling	485291.3	33855.44
Leaf Area	June	ambient	Cabernet Sauvignon	32.67344	1.6652732
			Riesling	37.15656	1.2179319
		elevated	Cabernet Sauvignon	31.075	1.2239788
			Riesling	40.76878	1.8667579
	August	ambient	Cabernet Sauvignon	16.32222	1.0871443
			Riesling	15.92222	1.3969985
		elevated	Cabernet Sauvignon	16.24444	1.3662714
			Riesling	14.9125	0.8105196
Leaf Weight	June	ambient	Cabernet Sauvignon	1225.7778	63.43219
			Riesling	1480.3444	61.04595
		elevated	Cabernet Sauvignon	1246.2111	87.92418
			Riesling	1564.2333	106.12474
	August	ambient	Cabernet Sauvignon	639.61	47.32213
			Riesling	729.1956	85.11076

		elevated	Cabernet Sauvignon	683.0133	75.83435
			Riesling	605.4056	46.61213
Porosity	June	ambient	Cabernet Sauvignon	0.99729	1.88E-04
			Riesling	0.9970026	3.16E-04
		elevated	Cabernet Sauvignon	0.9968796	2.52E-04
			Riesling	0.9966716	3.63E-04
	August	ambient	Cabernet Sauvignon	0.9966179	2.52E-04
			Riesling	0.996725	6.81E-05
		elevated	Cabernet Sauvignon	0.9970322	1.02E-04
			Riesling	0.9970619	8.39E-05
VoFrPa	June	ambient	Cabernet Sauvignon	0.001269633	1.03E-04
			Riesling	0.001355482	2.13E-04
		elevated	Cabernet Sauvignon	0.001425546	1.45E-04
			Riesling	0.001477189	1.69E-04
	August	ambient	Cabernet Sauvignon	0.001802242	1.47E-04
			Riesling	0.001826526	3.81E-05
		elevated	Cabernet Sauvignon	0.001632534	8.27E-05
			Riesling	0.001642634	4.49E-05
VoFrSp	June	ambient	Cabernet Sauvignon	0.001511384	1.39E-04
			Riesling	0.001586528	2.32E-04
		elevated	Cabernet Sauvignon	0.001630009	2.07E-04
			Riesling	0.001797955	1.88E-04
	August	ambient	Cabernet Sauvignon	0.001491246	1.27E-04
			Riesling	0.001437195	2.69E-05
		elevated	Cabernet Sauvignon	0.001300793	6.08E-05

			Riesling	0.001296184	2.87E-05
$V_c$max	June	ambient	Cabernet Sauvignon	79.40359	3.16119
			Riesling	85.36343	4.986907
		elevated	Cabernet Sauvignon	78.99067	4.7103
			Riesling	79.6674	3.101795
	August	ambient	Cabernet Sauvignon	65.59899	1.899492
			Riesling	70.95558	4.147718
		elevated	Cabernet Sauvignon	58.82802	3.435014
			Riesling	62.85625	2.63132
Jmax	June	ambient	Cabernet Sauvignon	196.6589	10.014375
			Riesling	216.8667	13.737537
		elevated	Cabernet Sauvignon	196.9847	9.530256
			Riesling	193.7517	5.970886
	August	ambient	Cabernet Sauvignon	114.9065	3.801626
			Riesling	137.077	9.755447
		elevated	Cabernet Sauvignon	116.0845	8.35216
			Riesling	118.3184	6.189272
Amax	June	ambient	Cabernet Sauvignon	43.05076	1.4239312
			Riesling	44.12494	1.806783
		elevated	Cabernet Sauvignon	43.73914	1.5986025
			Riesling	42.15923	1.4958549
	August	ambient	Cabernet Sauvignon	26.72096	0.6302933
			Riesling	30.57831	1.7034859
		elevated	Cabernet Sauvignon	27.34733	1.7109759
			Riesling	28.33745	1.4167898

gm	June	ambient	Cabernet Sauvignon	0.3821671	0.03322073
			Riesling	0.5246807	0.05004601
		elevated	Cabernet Sauvignon	0.4268688	0.0191792
			Riesling	0.4383978	0.03858675
	August	ambient	Cabernet Sauvignon	0.3578154	0.05167458
			Riesling	0.460442	0.04319371
		elevated	Cabernet Sauvignon	0.3740417	0.0463707
			Riesling	0.349466	0.03866981
SLA	June	ambient	Cabernet Sauvignon	0.02670581	0.000418747
			Riesling	0.02518914	0.0004604353
		elevated	Cabernet Sauvignon	0.02547793	0.001187442
			Riesling	0.02658778	0.0012528788
	August	ambient	Cabernet Sauvignon	0.0260089	0.0016110236
			Riesling	0.02243226	0.000945262
		elevated	Cabernet Sauvignon	0.02434217	0.0008644697
			Riesling	0.02400642	0.0009925028

Figures

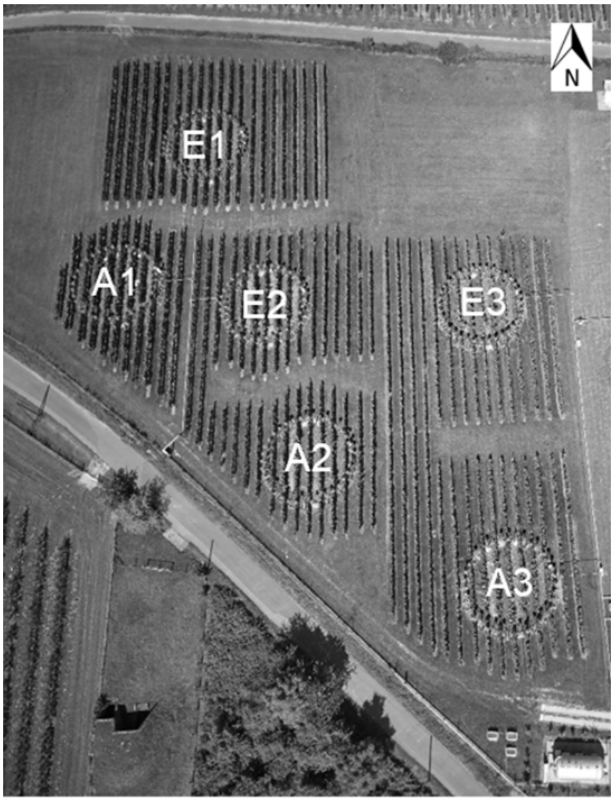

Figure 1. VineyardFACE experimental site at Hochschule Geisenheim University with associated CO_2 tank. Three FACE-rings were assigned to the two CO_2 levels aCO_2 (A1, A2 and A3) and eCO_2 (E1, E2 and E3).

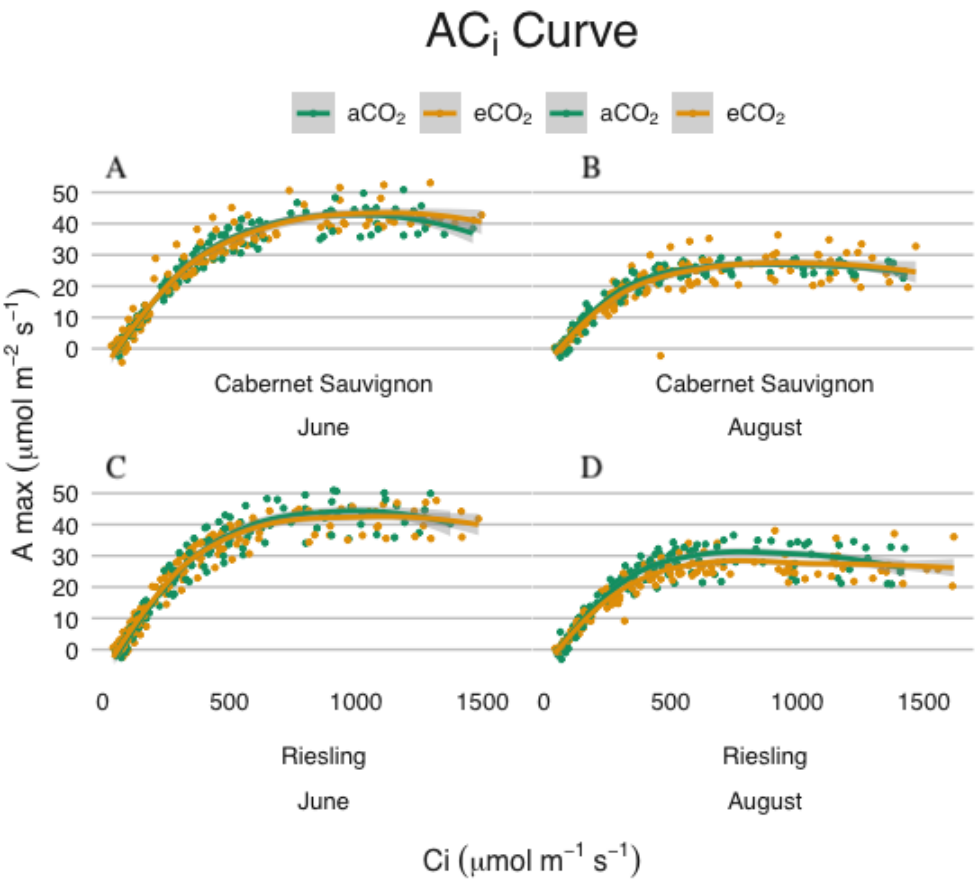

Fig. 2. Photosynthetic response curves (ACi curves) of *Vitis vinifera* cv. Cabernet Sauvignon and Riesling in June and August by CO_2 treatment effect. aCO_2 is ambient CO_2 (green) and eCO_2 represents elevated CO_2 (yellow).

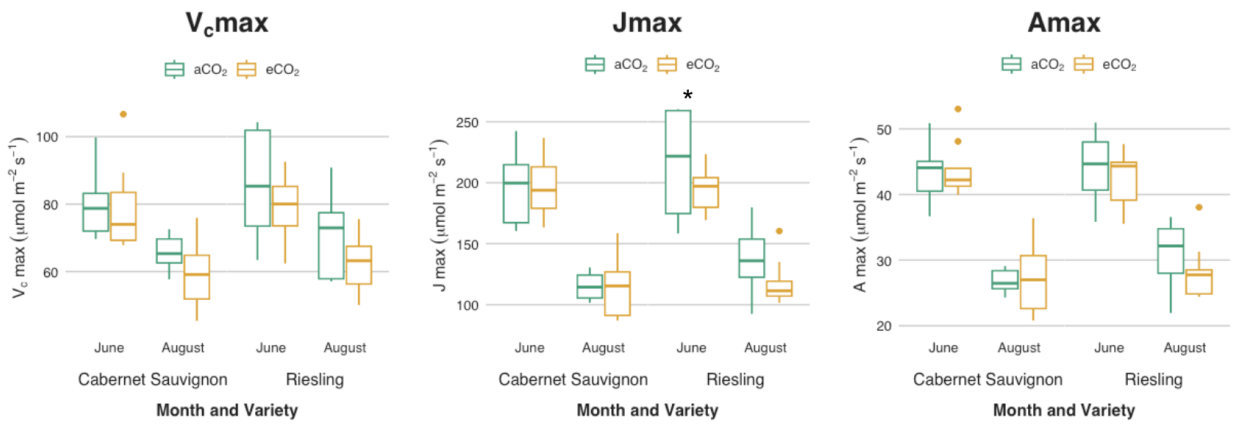

Fig. 3. Maximum rubisco carboxylation rate ($V_c$max), maximum electron transport rate (Jmax), and maximum photosynthetic rate (Amax) of *Vitis vinifera* cv. Cabernet Sauvignon (Cab Sauv) and Riesling in June and August. * indicates statistical significance ($p<0.1$) of main factor treatment.

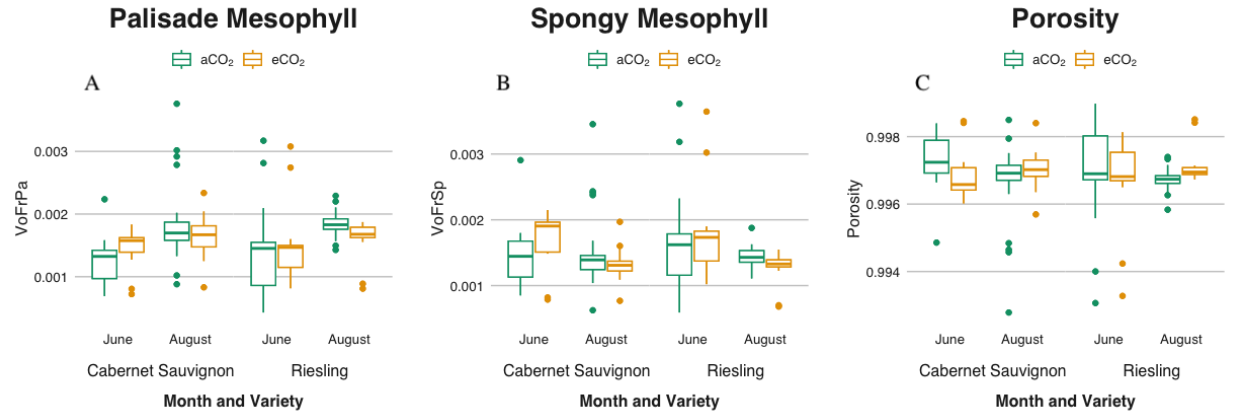

Fig. 4. A (left), B (middle), C (right). The fraction of palisade cell volume in total mesophyll volume (Palisade Mesophyll), the fraction of spongy cell volume in total mesophyll volume (Spongy Mesophyll), and the intercellular airspace volume to total volume ratio (porosity) of

Vitis vinifera cv. Cabernet Sauvignon and Riesling in June and August. * and ** indicate statistical significance ($p < 0.1$, $p < 0.01$) of main factor treatment.

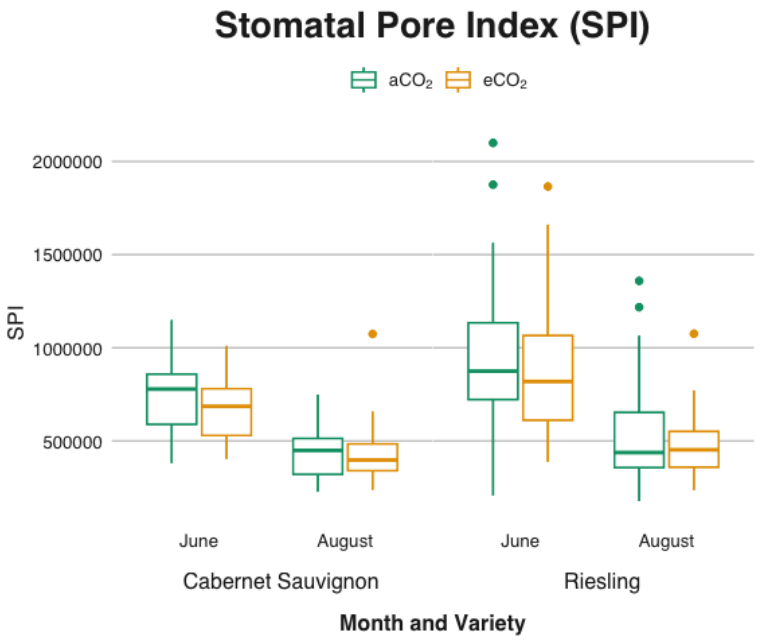

Fig. 5. Stomatal pore index (SPI) of *Vitis vinifera* cv. Cabernet Sauvignon (Cab Sauv) and Riesling in June and August. No significant differences of main factor treatment.

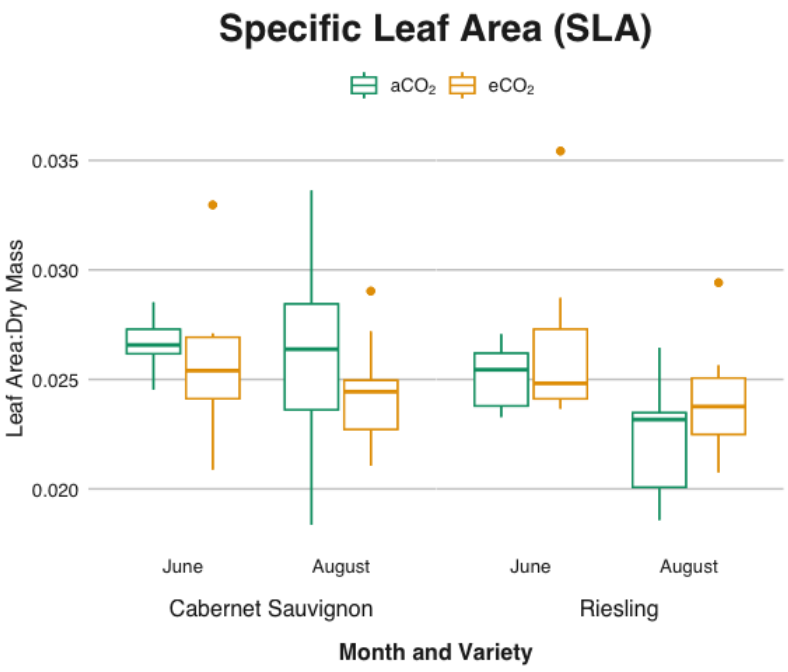

Fig. 6. Specific leaf area (SLA) of *Vitis vinifera* cv. Cabernet Sauvignon (Cab Sauv) and Riesling in June and August. No significant differences of main factor treatment.

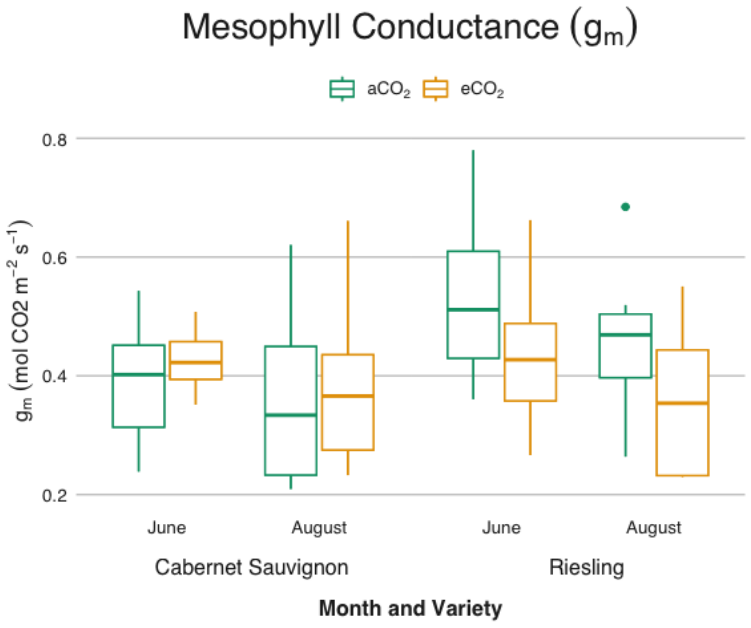

Fig. 7. Mesophyll conductance (g_m) of *Vitis vinifera* cv. Cabernet Sauvignon and Riesling in June

and August. No significant differences of main factor treatment.

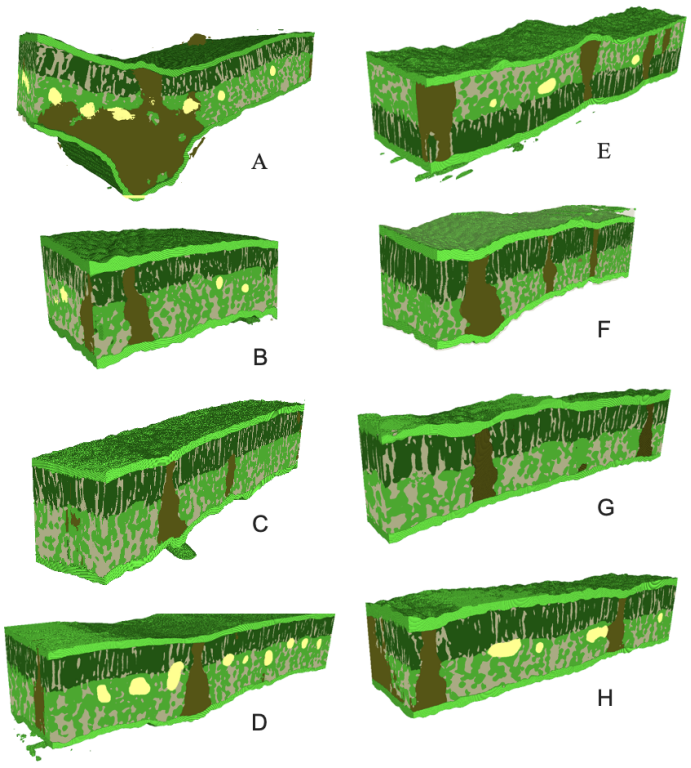

Fig. 8. MicroCT reconstructions of *Vitis vinifera* cv. Cabernet Sauvignon. and Riesling in June (A-D left column) and August (E-H right column). A/E, B/F, C/G, and D/H represent the same vines at two time points in the season. A & E are from an aCO_2 Riesling vine, B & F are eCO_2 Riesling, C & G are aCO_2 Cabernet Sauvignon, and D & H are eCO_2 Cabernet Sauvignon.

Supplemental

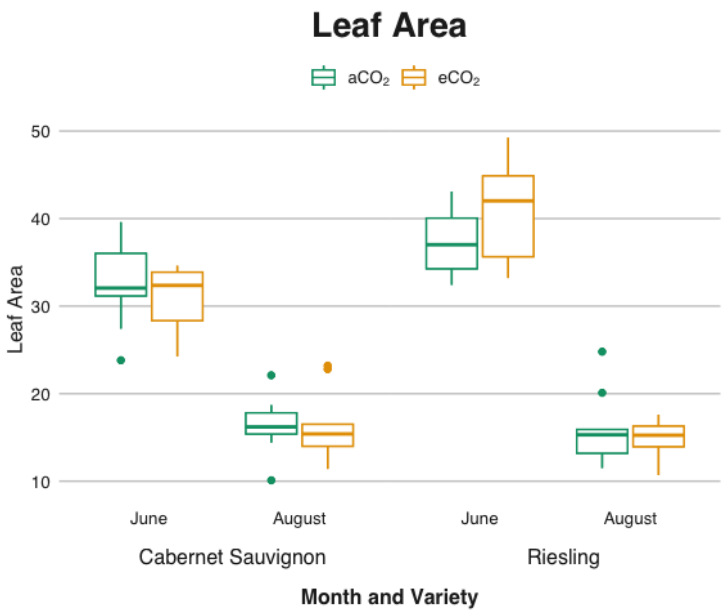

Fig. 9. Leaf area of *Vitis vinifera* cv. Cabernet Sauvignon. and Riesling in June and August. No significant differences of main factor treatment.

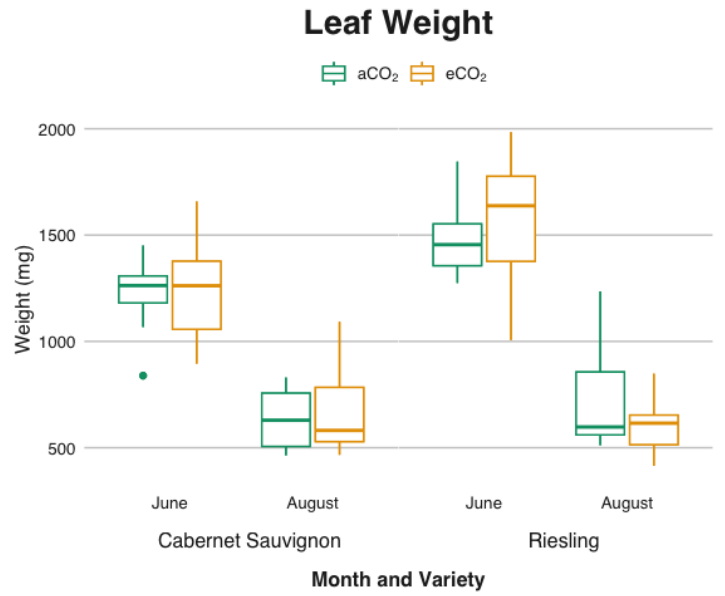

Fig. 10. Leaf weight of *Vitis vinifera* cv. Cabernet Sauvignon. and Riesling in June and August. No significant differences of main factor treatment.

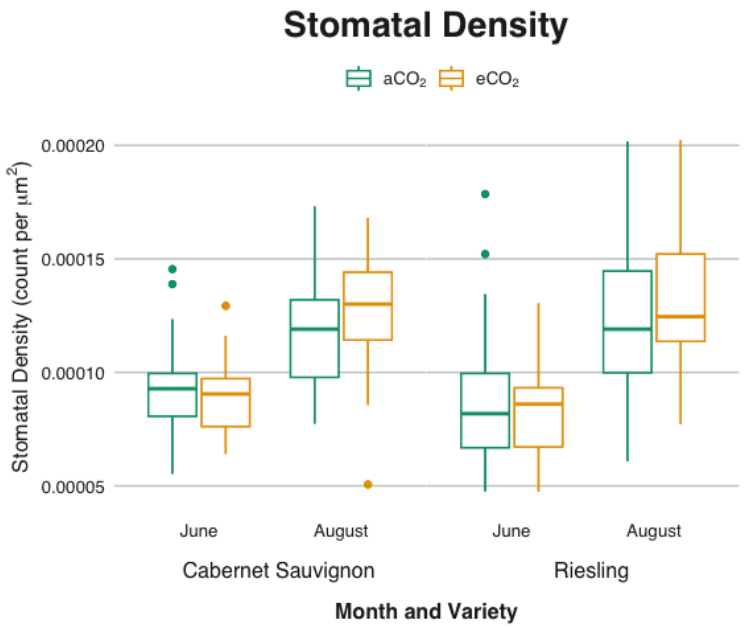

Fig. 11. Stomatal density of *Vitis vinifera* cv. Cabernet Sauvignon. and Riesling in June and August. No significant differences of main factor treatment.

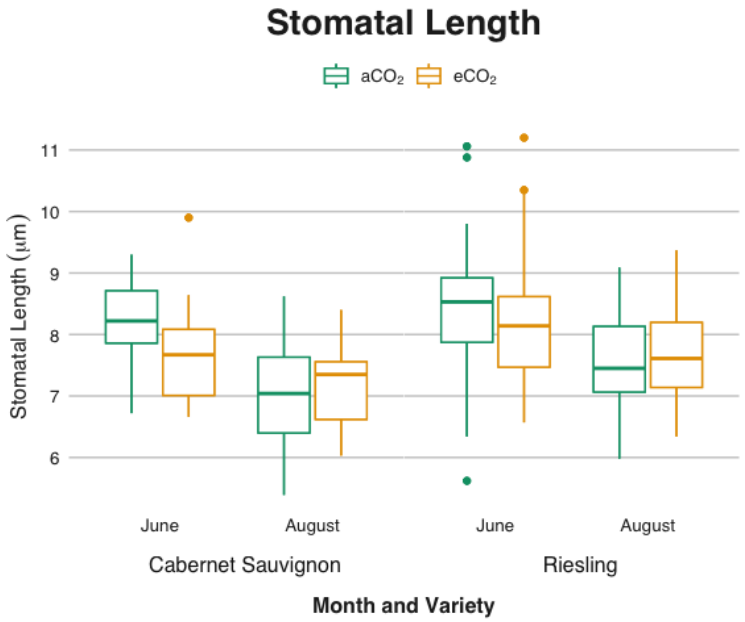

Fig. 12. Stomatal length of *Vitis vinifera* cv. Cabernet Sauvignon. and Riesling in June and August. No significant differences of main factor treatment.

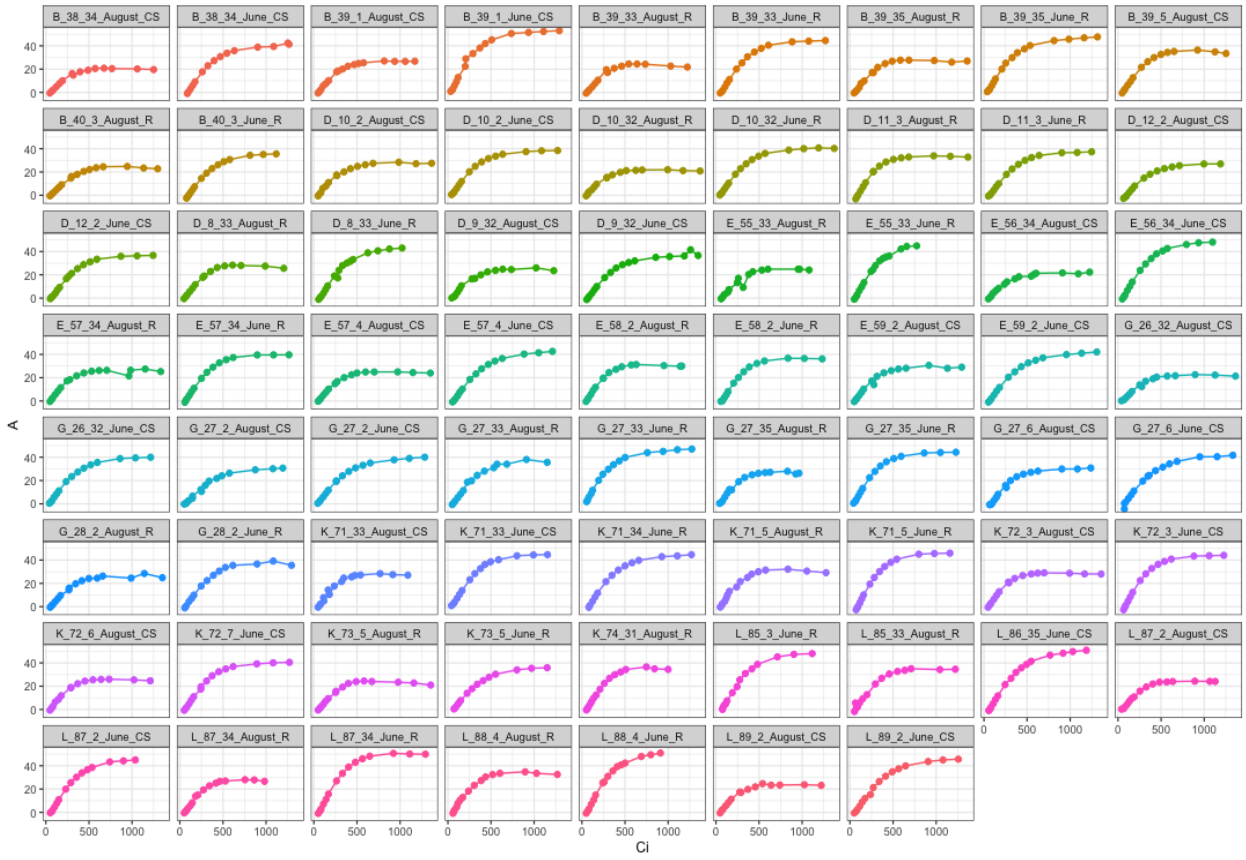

Fig. 13. Individual photosynthetic response curves (ACi curves) of *Vitis vinifera* cv. Cabernet Sauvignon and Riesling in June and August by CO_2 treatment effect. aCO_2 is ambient CO_2 and eCO_2 represents elevated CO_2.

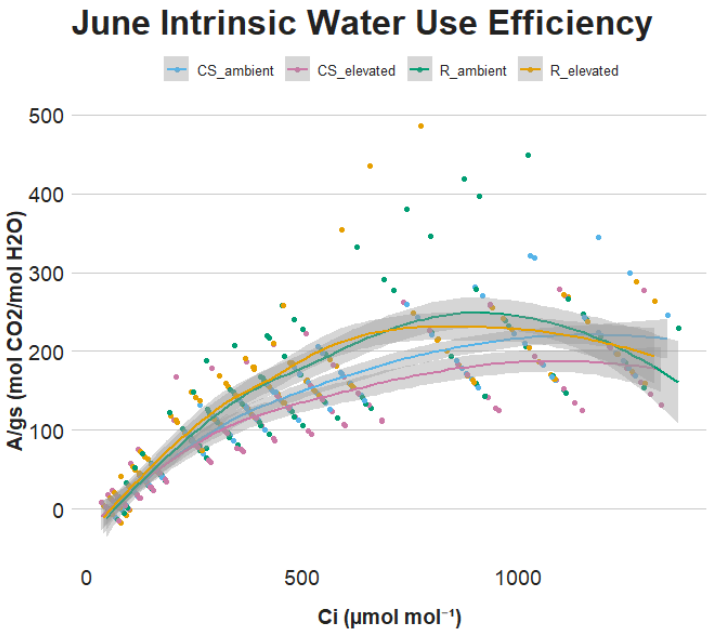

Fig. 14. Intrinsic water use efficiency of *Vitis vinifera* cv. Cabernet Sauvignon. and Riesling in June. No significant differences of main factor treatment.

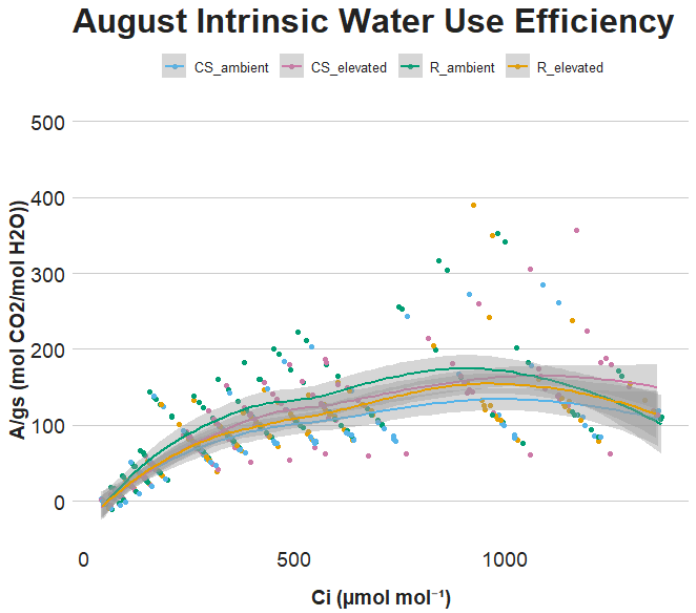

Fig. 15. Intrinsic water use efficiency of *Vitis vinifera* cv. Cabernet Sauvignon. and Riesling in August. No significant differences of main factor treatment.

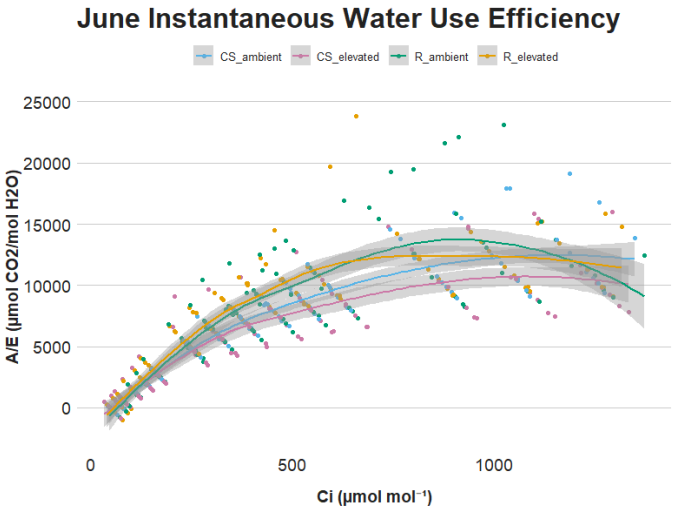

Fig. 16. Instantaneous water use efficiency of *Vitis vinifera* cv. Cabernet Sauvignon. and Riesling in June. No significant differences of main factor treatment.

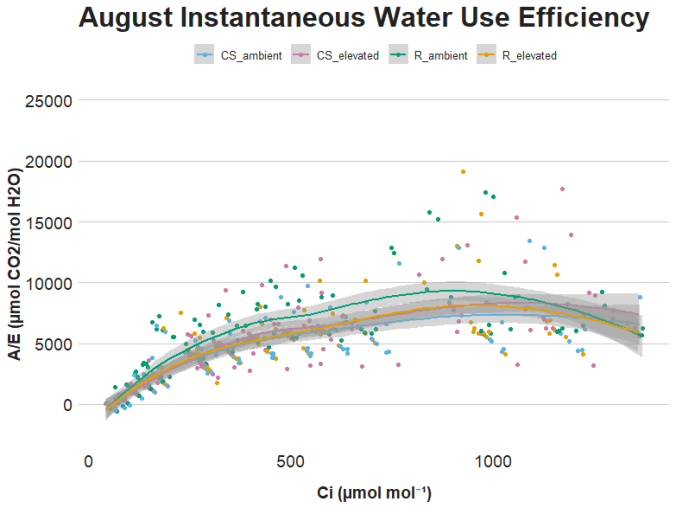

Fig. 17. Instantaneous water use efficiency of *Vitis vinifera* cv. Cabernet Sauvignon. and Riesling in August. No significant differences of main factor treatment.

References

Ainsworth, Elizabeth A., and Stephen P. Long. 2021. “30 Years of Free-Air Carbon Dioxide Enrichment (FACE): What Have We Learned about Future Crop Productivity and Its Potential for Adaptation?” *Global Change Biology* 27 (1): 27–49.

Ainsworth, Elizabeth A., and Alistair Rogers. 2007. “The Response of Photosynthesis and Stomatal Conductance to Rising [CO_2]: Mechanisms and Environmental Interactions.” *Plant, Cell & Environment* 30 (3): 258–70.

Ainsworth, Elizabeth A., and Stephen P. Long. 2005. “What Have We Learned from 15 Years of Free-Air CO_2 Enrichment (FACE)? A Meta-Analytic Review of the Responses of Photosynthesis, Canopy Properties and Plant Production to Rising CO_2.” *The New Phytologist* 165 (2): 351–71.

Allen, L. H., and Marian K. Viney. “Advances in Carbon Dioxide Effects Research : Proceedings of a Symposium.” Madison, Wis: American Society of Agronomy, 1997. Print.

Allen, L. H., B. A. Kimball, J. A. Bunce, M. Yoshimoto, Y. Harazono, J. T. Baker, K. J. Boote, and J. W. White. 2020. “Fluctuations of CO_2 in Free-Air CO_2 Enrichment (FACE) Depress Plant Photosynthesis, Growth, and Yield.” *Agricultural and Forest Meteorology* 284 (April): 107899.

Apel, P. 1989. “Influence of CO_2 on Stomatal Numbers.” *Biologia Plantarum* 31 (1): 72–74.

Bindi, M., L. Fibbi, and F. Miglietta. 2001. “Free Air CO_2 Enrichment (FACE) of Grapevine (Vitis Vinifera L.): II. Growth and Quality of Grape and Wine in Response to Elevated CO_2 Concentrations.” *European Journal of Agronomy: The Journal of the European Society for Agronomy* 14 (2): 145–55.

Bindi, M., L. Fibbi, M. Lanini, and F. Miglietta. 2001. “Free Air CO_2 Enrichment (FACE) of Grapevine (Vitis Vinifera L.): I. Development and Testing of the System for CO_2 Enrichment.” *European Journal of Agronomy: The Journal of the European Society for Agronomy* 14 (2): 135–43.

Bindi, Marco, Antonio Raschi, Mario Lanini, Francesco Miglietta, and Roberto Tognetti. 2005. "Physiological and Yield Responses of Grapevine (Vitis Vinifera L.) Exposed to Elevated CO_2 Concentrations in a Free Air CO_2 Enrichment (FACE)." *Journal of Crop Improvement* 13 (1-2): 345–59.

Bindi M, Fibbi L, Miglietta F. 2001. Free Air CO_2 Enrichment (FACE) of grapevine (*Vitis vinifera* L.). II. Growth and quality of grape and wine in response to elevated CO_2 concentrations. *European Journal of Agronomy* 14: 145– 155.

California Department of Food, and Agriculture. n.d. "CDFA - Statistics." Accessed February 19, 2023. https://www.cdfa.ca.gov/statistics/.

Canadell, Josep G. 2006. *A Guide to Establish Free Air CO_2 Enrichment (FACE) Experimentation: Annual Cropping in Australia : Technical Report*. Australian Greenhouse Office.

Clemens, Molly E., Alessandra Zuniga, and Walter Oechel. 2021. "The Effects of Elevated Atmospheric Carbon Dioxide on the Vineyard System of Vitis Vinifera: A Review." *American Journal of Enology and Viticulture*, November. https://doi.org/10.5344/ajev.2021.21029.

Dawes, Melissa A., Frank Hagedorn, Ira Tanya Handa, Kathrin Streit, Alf Ekblad, Christian Rixen, Christian Körner, and Stephan Hättenschwiler. 2013. "An Alpine Treeline in a Carbon Dioxide-Rich World: Synthesis of a Nine-Year Free-Air Carbon Dioxide Enrichment Study." *Oecologia* 171 (3): 623–37.

Earles, J. Mason, Guillaume Theroux-Rancourt, Adam B. Roddy, Matthew E. Gilbert, Andrew J. McElrone, and Craig R. Brodersen. 2018. “Beyond Porosity: 3D Leaf Intercellular Airspace Traits That Impact Mesophyll Conductance.” *Plant Physiology* 178 (1): 148–62.

Erda, Lin, Xiong Wei, Ju Hui, Xu Yinlong, Li Yue, Bai Liping, and Xie Liyong. 2005. “Climate Change Impacts on Crop Yield and Quality with CO_2 Fertilization in China.” *Philosophical Transactions of the Royal Society of London. Series B, Biological Sciences* 360 (1463): 2149–54.

Field, Christopher B., J. Timothy Ball, and Joseph A. Berry. 2000. “Photosynthesis: Principles and Field Techniques.” *Plant Physiological Ecology*. https://doi.org/10.1007/978-94-010-9013-1_11.

Flexas, Jaume, Miquel Ribas-Carbó, Antonio Díaz-Espejo, Jeroni Galmés, and Hipólito Medrano. 2008. “Mesophyll Conductance to CO_2: Current Knowledge and Future Prospects.” *Plant, Cell & Environment* 31 (5): 602–21.

Franks, Peter J., and David J. Beerling. 2009. “Maximum Leaf Conductance Driven by CO_2 Effects on Stomatal Size and Density over Geologic Time.” *Proceedings of the National Academy of Sciences of the United States of America* 106 (25): 10343–47.

Garnier, E., B. Shipley, C. Roumet, and G. Laurent. 2001. “A Standardized Protocol for the Determination of Specific Leaf Area and Leaf Dry Matter Content.” *Functional Ecology* 15 (5): 688–95.

Gonçalves, Berta, Virgílio Falco, José Moutinho-Pereira, Eunice Bacelar, Francisco Peixoto, and Carlos Correia. 2009a. “Effects of Elevated CO_2 on Grapevine (Vitis Vinifera L.): Volatile

Composition, Phenolic Content, and in Vitro Antioxidant Activity of Red Wine." *Journal of Agricultural and Food Chemistry* 57 (1): 265–73.

Harley, P. C., F. Loreto, G. Di Marco, and T. D. Sharkey. 1992. "Theoretical Considerations When Estimating the Mesophyll Conductance to CO(2) Flux by Analysis of the Response of Photosynthesis to CO(2)." *Plant Physiology* 98 (4): 1429–36.

Hendrey, George. 1992. *FACE Free Air CO_2 Enrichment Plant Research in the Field*. CRC-Press.

International Organisation of Vine and Wine Annual Assessment of World Vine and Wine Sector 2021. https://www.oiv.int/sites/default/files/documents/OIV_Annual_Assessment_of_the_World_Vine_and_Wine_Sector_in_2021.pdf

IPCC. 2014. "Climate Change 2014 Synthesis Report." *IPCC: Geneva, Szwitzerland*. ftp://atitlan.ethz.ch/docs/afischli/for-srinivasan/TS-01978822-Can't%20suppress%20pdf%20indexing%20during%20imports/Attached%20PDFs/Ip096.pdf.

Jones, Gregory V., Michael A. White, Owen R. Cooper, and Karl Storchmann. 2005. "Climate Change and Global Wine Quality." *Climatic Change* 73 (3): 319–43.

Kimball, B. A., K. Kobayashi, and M. Bindi. 2002. "Responses of Agricultural Crops to Free-Air CO_2 Enrichment." In *Advances in Agronomy*, edited by Donald L. Sparks, 77:293–368. Academic Press.

Kimball, Bruce A., Paul J. Pinter, Richard L. Garcia, Robert L. LaMORTE, Gerard W. Wall, Douglas J. Hunsaker, Gabriele Wechsung, Frank Wechsung, and Thomas KARTSCHALLs. 1995. "Productivity and Water Use of Wheat under Free-Air CO_2 Enrichment." *Global Change Biology* 1 (6): 429–42.

Kizildeniz, T., J. J. Irigoyen, I. Pascual, and F. Morales. 2018. "Simulating the Impact of Climate Change (Elevated CO_2 and Temperature, and Water Deficit) on the Growth of Red and White Tempranillo Grapevine in Three Consecutive Growing Seasons (2013–2015)." *Agricultural Water Management* 202 (April): 220–30.

Krishnan, P., D. K. Swain, B. Chandra Bhaskar, S. K. Nayak, and R. N. Dash. 2007. "Impact of Elevated CO_2 and Temperature on Rice Yield and Methods of Adaptation as Evaluated by Crop Simulation Studies." *Agriculture, Ecosystems & Environment* 122 (2): 233–42.

Leakey, Andrew D. B., Martin Uribelarrea, Elizabeth A. Ainsworth, Shawna L. Naidu, Alistair Rogers, Donald R. Ort, and Stephen P. Long. 2006. "Photosynthesis, Productivity, and Yield of Maize Are Not Affected by Open-Air Elevation of CO_2 Concentration in the Absence of Drought." *Plant Physiology* 140 (2): 779–90.

Leakey, Andrew D. B., Elizabeth A. Ainsworth, Carl J. Bernacchi, Alistair Rogers, Stephen P. Long, and Donald R. Ort. 2009. "Elevated CO2 Effects on Plant Carbon, Nitrogen, and Water Relations: Six Important Lessons from FACE." *Journal of Experimental Botany* 60 (10): 2859–76.

Leakey, Andrew D. B., Elizabeth A. Ainsworth, Carl J. Bernacchi, Xinguang Zhu, Stephen P. Long, and Donald R. Ort. 2012. "Photosynthesis in a CO_2-Rich Atmosphere." In *Photosynthesis:*

Plastid Biology, Energy Conversion and Carbon Assimilation, edited by Julian J. Eaton-Rye, Baishnab C. Tripathy, and Thomas D. Sharkey, 733–68. Dordrecht: Springer Netherlands.

Lobell, D., and M. Burke. 2010. "Economic Impacts of Climate Change on Agriculture to 2030." *Climate Change and Crop Production*. https://doi.org/10.1079/9781845936334.0038.

Lobell, David B., Christopher B. Field, Kimberly Nicholas Cahill, and Celine Bonfils. 2006. "Impacts of Future Climate Change on California Perennial Crop Yields: Model Projections with Climate and Crop Uncertainties." *Agricultural and Forest Meteorology*. https://doi.org/10.1016/j.agrformet.2006.10.006.

Long, Farage, and Garcia. n.d. "Measurement of Leaf and Canopy Photosynthetic C02 Exchange in the field1." *Journal of Experimental Botany*. https://academic.oup.com/jxb/article/47/11/1629/600322.

Long, Stephen P., Elizabeth A. Ainsworth, Andrew D. B. Leakey, Josef Nösberger, and Donald R. Ort. 2006. "Food for Thought: Lower-than-Expected Crop Yield Stimulation with Rising CO_2 Concentrations." *Science* 312 (5782): 1918–21.

Miglietta, F., V. Magliulo, M. Bindi, L. Cerio, F. P. Vaccari, V. Loduca, and A. Peressotti. 1998. "Free Air CO 2 Enrichment of Potato (Solanum Tuberosum L.): Development, Growth and Yield." *Global Change Biology* 4 (2): 163–72.

Miglietta, Franco, Alessandro Peressotti, Francesco Primo Vaccari, Alessandro Zaldei, Paolo DeAngelis, and Giuseppe Scarascia-Mugnozza. 2001. "Free-Air CO_2 Enrichment (FACE) of a Poplar Plantation: The POPFACE Fumigation System." *The New Phytologist* 150 (2): 465–76.

Mizokami, Yusuke, Daisuke Sugiura, Chihiro K. A. Watanabe, Eriko Betsuyaku, Noriko Inada, and Ichiro Terashima. 2019. “Elevated CO2-Induced Changes in Mesophyll Conductance and Anatomical Traits in Wild Type and Carbohydrate-Metabolism Mutants of Arabidopsis.” *Journal of Experimental Botany* 70 (18): 4807–18.

Mollah, Mahabubur R., Dale J. Unwin, Glenn J. Fitzgerald, and Everard J. Edwards. 2018. “A CO_2 Injection System inside an Open-Top Chamber Enclosing Mature Field-Grown Grapevines: Design and Performance.” *Transactions of the ASABE* 61 (4): 1231–39.

Momayyezi, Mina, Aleca M. Borsuk, Craig R. Brodersen, Matthew E. Gilbert, Guillaume Théroux-Rancourt, Daniel A. Kluepfel, and Andrew J. McElrone. 2022. “Desiccation of the Leaf Mesophyll and Its Implications for CO_2 Diffusion and Light Processing.” *Plant, Cell & Environment* 45 (5): 1362–81.

Moutinho-Pereira, J., Berta Gonçalves, Eunice Bacelar, J. Boaventura Cunha, J. Countinho, and C. M. Correira. 2015. “Effects of Elevated CO_2 on Grapevine (Vitis Vinifera L.): Physiological and Yield Attributes.” *Vitis-Journal of Grapevine Research* 48 (4): 159.

Norby, Richard J., and Donald R. Zak. 2011. “Ecological Lessons from Free-Air CO_2 Enrichment (FACE) Experiments.” *Annual Review of Ecology, Evolution, and Systematics* 42 (1): 181–203.

Ogaya, Romá, L. Llorens, and Josep Peñuelas. 2011. “Density and Length of Stomatal and Epidermal Cells in‘ Living Fossil’ Trees Grown under Elevated CO2 and a Polar Light Regime.” *Acta Oecologica* 37 (4): 381–85.

Poorter, Hendrik, Oliver Knopf, Ian J. Wright, Andries A. Temme, Sander W. Hogewoning, Alexander Graf, Lucas A. Cernusak, and Thijs L. Pons. 2022. “A Meta-Analysis of Responses of C3 Plants to Atmospheric CO_2 : Dose-Response Curves for 85 Traits Ranging from the Molecular to the Whole-Plant Level.” *The New Phytologist* 233 (4): 1560–96.

Pritchard, Seth G., Hugo H. Rogers, Stephen A. Prior, and Curt M. Peterson. 1999. “Elevated CO_2 and Plant Structure: A Review.” *Global Change Biology* 5 (7): 807–37.

Purcell, C., S. P. Batke, C. Yiotis, R. Caballero, W. K. Soh, M. Murray, and J. C. McElwain. 2018. “Increasing Stomatal Conductance in Response to Rising Atmospheric CO_2.” *Annals of Botany* 121 (7): 1427.

Real, António C., José Borges, J. Sarsfield Cabral, and Gregory V. Jones. 2015. “Partitioning the Grapevine Growing Season in the Douro Valley of Portugal: Accumulated Heat Better than Calendar Dates.” *International Journal of Biometeorology* 59 (8): 1045–59.

Reid, Chantal D. 2003. “On the Relationship between Stomatal Characters and Atmospheric CO_2.” *Geophysical Research Letters* 30 (19). https://doi.org/10.1029/2003gl017775.

Rippner, Devin A., Pranav V. Raja, J. Mason Earles, Mina Momayyezi, Alexander Buchko, Fiona V. Duong, Elizabeth J. Forrestel, et al. 2022. “A Workflow for Segmenting Soil and Plant X-Ray Computed Tomography Images with Deep Learning in Google’s Colaboratory.” *Frontiers in Plant Science* 13 (September): 893140.

Rippner D, Raja P, Earles J, Momayyezi M, Buchko A, Duong F, Forrestel E, Parkinson D, Shackel K, and Neyhart J (2022) A workflow for segmenting soil and plant X-ray computed tomography images with deep learning in Google’s Colaboratory. Front. Plant Sci. 13: 893140.

Robana, Rubi. 1996. *Impact of Temperature and Atmospheric CO_2 Enrichment on Cotton Growth and Leaf Morphology*. Mississippi State University. Department of Plant and Soil Sciences.

Roderick, Michael L., Sandra L. Berry, and Ian R. Noble. 1999. "The Relationship between Leaf Composition and Morphology at Elevated CO_2 Concentrations." *The New Phytologist* 143 (1): 63–72.

Rosado-Porto, David, Stefan Ratering, Yvette Wohlfahrt, Bellinda Schneider, Andrea Glatt, and Sylvia Schnell. 2023. "Elevated Atmospheric CO_2 Concentrations Caused a Shift of the Metabolically Active Microbiome in Vineyard Soil." *BMC Microbiology* 23 (1): 46.

Royer, D. L. 2001. "Stomatal Density and Stomatal Index as Indicators of Paleoatmospheric CO_2 Concentration." *Review of Palaeobotany and Palynology* 114 (1): 1–28.

Sage, Rose. 1990. "A Model Describing the Regulation of Ribulose-1, 5-Bisphosphate Carboxylase, Electron Transport, and Triose Phosphate Use in Response to Light Intensity and CO2 in C3 …." n.d. https://academic.oup.com/plphys/article-abstract/94/4/1728/6086209.

Salazar-Parra, Carolina, Iker Aranjuelo, Inmaculada Pascual, Gorka Erice, Álvaro Sanz-Sáez, Jone Aguirreolea, Manuel Sánchez-Díaz, Juan José Irigoyen, José Luis Araus, and Fermín Morales. 2015. "Carbon Balance, Partitioning and Photosynthetic Acclimation in Fruit-Bearing Grapevine (Vitis Vinifera L. Cv. Tempranillo) Grown under Simulated Climate Change (elevated CO_2, Elevated Temperature and Moderate Drought) Scenarios in Temperature Gradient Greenhouses." *Journal of Plant Physiology* 174: 97–109.

Sasek, Thomas W., and Boyd R. Strain. 1991. “Effects of Co 2 Enrichment on the Growth and Morphology of a Native and an Introduced Honeysuckle Vine.” *American Journal of Botany* 78 (1): 69–75.

Schulze-Sylvester, Maria, and Annette Reineke. 2019. “Elevated CO_2 Levels Impact Fitness Traits of Vine Mealybug Planococcus Ficus Signoret, but Not Its Parasitoid Leptomastix Dactylopii Howard.” *Agronomy* 9 (6): 326.

Schultz, Hans R. 2003. “Extension of a Farquhar Model for Limitations of Leaf Photosynthesis Induced by Light Environment, Phenology and Leaf Age in Grapevines (Vitis Vinifera L. Cvv. White Riesling and Zinfandel).” *Functional Plant Biology: FPB* 30 (6): 673–87.

Seibt, Ulli, Abazar Rajabi, Howard Griffiths, and Joseph A. Berry. 2008. “Carbon Isotopes and Water Use Efficiency: Sense and Sensitivity.” *Oecologia* 155 (3): 441–54.

Sharkey, Thomas D., Carl J. Bernacchi, Graham D. Farquhar, and Eric L. Singsaas. 2007. “Fitting Photosynthetic Carbon Dioxide Response Curves for C(3) Leaves.” *Plant, Cell & Environment* 30 (9): 1035–40.

Sharkey, Thomas D. 2016. “What Gas Exchange Data Can Tell Us about Photosynthesis.” *Plant, Cell & Environment*.

Shen, Min, Chuang Cai, Lian Song, Jiangbo Qiu, Chuanqi Ma, Dongming Wang, Xinyue Gu, et al. 2023. “Elevated CO_2 and Temperature under Future Climate Change Increase Severity of Rice Sheath Blight.” *Frontiers in Plant Science* 14 (January): 1115614.

Silvestroni, O., S. Mattioli, D. Neri, A. Palliotti, and A. Cartechini. 2004. “Down-Regulation of Photosynthetic Activity for Field-Grown Grapevines.” In *VII International Symposium on Grapevine Physiology and Biotechnology 689*, 285–92.

Sinha, P. G., and A. K. Bhatnagar. 2014. “Effect of Elevated [CO_2] on Cell Structure and Function in Seed Plants.” *Change and Environmental.* https://www.indianjournals.com/ijor.aspx?target=ijor:cces&volume=2&issue=2&article=001.

Théroux‐Rancourt, Guillaume., and M. R. Jenkins. 2020. “Digitally Deconstructing Leaves in 3D Using X‐ray Microcomputed Tomography and Machine Learning.” *Applications in Plant Sciences*. https://bsapubs.onlinelibrary.wiley.com/doi/abs/10.1002/aps3.11380.

Théroux-Rancourt Guillaume, Herrera C, Voggeneder K, Luijken N, Nocker L, Savi T, Scheffknecht S, Schneck M, Tholen D. (accepted) “Analyzing anatomy over three dimensions unpacks the differences in mesophyll diffusive area between sun and shade Vitis vinifera leaves.” AoB Plants

Théroux-Rancourt, Guillaume, Adam B. Roddy, J. Mason Earles, Matthew E. Gilbert, Maciej A. Zwieniecki, C. Kevin Boyce, Danny Tholen, Andrew J. McElrone, Kevin A. Simonin, and Craig R. Brodersen. 2021. “Maximum CO_2 Diffusion inside Leaves Is Limited by the Scaling of Cell Size and Genome Size.” *Proceedings. Biological Sciences / The Royal Society* 288 (1945): 20203145.

Théroux‐Rancourt, Guillaume, J. Mason Earles, Matthew E. Gilbert, Maciej A. Zwieniecki, C. Kevin Boyce, Andrew J. McElrone, and Craig R. Brodersen. 2017. “The Bias of a

Two‐dimensional View: Comparing Two‐dimensional and Three‐dimensional Mesophyll Surface Area Estimates Using Noninvasive Imaging." *The New Phytologist* 215 (4): 1609–22.

Théroux-Rancourt, Guillaume, José Carlos Herrera, Klara Voggeneder, Federica De Berardinis, Natascha Luijken, Laura Nocker, Tadeja Savi, Susanne Scheffknecht, Moritz Schneck, and Danny Tholen. 2023. "Analyzing Anatomy over Three Dimensions Unpacks the Differences in Mesophyll Diffusive Area between Sun and Shade Vitis Vinifera Leaves." *AoB Plants*, January, lad001.

Tognetti, R., A. Raschi, A. Longobucco, M. Lanini, and M. Bindi. 2005. "Hydraulic Properties and Water Relations of Vitis Vinifera L. Exposed to Elevated CO\ 2 Concentrations in a Free Air CO\ 2 Enrichment (FACE)." *PHYTON-HORN*- 45 (3): 243.

Tomás, M., H. Medrano, E. Brugnoli, J. M. Escalona, S. Martorell, A. Pou, M. Ribas-Carbó, and J. Flexas. 2014. "Variability of Mesophyll Conductance in Grapevine Cultivars under Water Stress Conditions in Relation to Leaf Anatomy and Water Use Efficiency." *Australian Journal of Grape and Wine Research* 20 (2): 272–80.

Ueyama, Masahito, Kazuhito Ichii, Hideki Kobayashi, Tomo 'omi Kumagai, Jason Beringer, Lutz Merbold, Eugénie S. Euskirchen, et al. 2020. "Inferring CO2 Fertilization Effect Based on Global Monitoring Land-Atmosphere Exchange with a Theoretical Model." *Environmental Research Letters: ERL [Web Site]* 15 (8): 084009.

Walker, Anthony P., Andrew P. Beckerman, Lianhong Gu, Jens Kattge, Lucas A. Cernusak, Tomas F. Domingues, Joanna C. Scales, Georg Wohlfahrt, Stan D. Wullschleger, and F. Ian Woodward. 2014. "The Relationship of Leaf Photosynthetic Traits - V Cmax and J Max - to Leaf

Nitrogen, Leaf Phosphorus, and Specific Leaf Area: A Meta-Analysis and Modeling Study." *Ecology and Evolution* 4 (16): 3218–35.

Wohlfahrt, Y., J. P. Smith, S. Tittmann, B. Honermeier, and M. Stoll. 2018. "Primary Productivity and Physiological Responses of Vitis Vinifera L. Cvs. under Free Air Carbon Dioxide Enrichment (FACE)." *European Journal of Agronomy: The Journal of the European Society for Agronomy* 101 (November): 149–62.

Wohlfahrt, Y. et al. "Primary Productivity and Physiological Responses of Vitis Vinifera L. Cvs. Under Free Air Carbon Dioxide Enrichment (FACE)." European journal of agronomy 101 (2018): 149–162. Web.

Wohlfahrt, Yvette, Claus-Dieter Patz, Dominik Schmidt, Doris Rauhut, Bernd Honermeier, and Manfred Stoll. 2021. "Responses on Must and Wine Composition of Vitis Vinifera L. Cvs. Riesling and Cabernet Sauvignon under a Free Air CO_2 Enrichment (FACE)." *Foods (Basel, Switzerland)* 10 (1). https://doi.org/10.3390/foods10010145.

Wohlfahrt, Yvette, Katja Krüger, Daniel Papsdorf, Susanne Tittmann, and Manfred Stoll. 2022. "Grapevine Leaf Physiology and Morphological Characteristics to Elevated CO_2 in the VineyardFACE (Free Air Carbon Dioxide Enrichment) Experiment." *Frontiers in Plant Science* 13 (December): 1085878.

Wohlfahrt, Yvette, Susanne Tittmann, Dominik Schmidt, Doris Rauhut, Bernd Honermeier, and Manfred Stoll. 2020. "The Effect of Elevated CO_2 on Berry Development and Bunch Structure of Vitis Vinifera L. Cvs. Riesling and Cabernet Sauvignon." *NATO Advanced Science Institutes Series E: Applied Sciences* 10 (7): 2486.

Yahia, Elhadi M., Armando Carrillo-López, Guadalupe Malda Barrera, Humberto Suzán-Azpiri, and Mónica Queijeiro Bolaños. 2019. “Chapter 3 - Photosynthesis.” In *Postharvest Physiology and Biochemistry of Fruits and Vegetables*, edited by Elhadi M. Yahia, 47–72. Woodhead Publishing.

Zeiger, Eduardo, G. D. Farquhar, and I. R. Cowan. 1987. *Stomatal Function*. Stanford University Press.

Zhan, Chunhui, René Orth, Mirco Migliavacca, Sönke Zaehle, Markus Reichstein, Jan Engel, Anja Rammig, and Alexander J. Winkler. 2022. “Emergence of the Physiological Effects of Elevated CO_2 on Land-Atmosphere Exchange of Carbon and Water.” *Global Change Biology* 28 (24): 7313–26.